19th World Congress of Soil Science

Symposium 1.5.2
Modelling critical processes in changing soil

Soil Solutions for a Changing World,

Brisbane, Australia

1 – 6 August 2010

Table of Contents

Applicability of HYDRUS to predict soil moisture and temperature in vadose zone of arable land under monsoonal climate region, Tokyo

Chihiro Kato[A], Taku Nishimura[A], Hiromi Imoto[A] and Tsuyoshi Miyazaki[A]

[A]Graduate School of Agricultural and Life Sciences, University of Tokyo, Japan, Email kato@soil.en.a.u-tokyo.ac.jp

Abstract
In order to project effects of future climate change on the vadose zone, performance of HYDRUS ver 4.09 model, which had been mostly applied to dry regions (e.g. Saito *et al.* 2006), was tested for a monsoonal climate. We conducted analysis of simultaneous liquid water, vapor and heat transport across the border between atmosphere and vadose zone, and prediction of annual change in soil moisture and temperature of arable land in Tokyo. Besides, we monitored soil temperature and soil moisture and made a dataset for model validation. In the simulation, soil hydraulic and thermal parameters were obtained by laboratory experiments. Meteorological data being open to the public had been used for input data for boundary condition. The simulation in general represented the monitored data well. The HYDRUS model could be considered appropriate proper and reasonable for the future use in the monsoonal climate region.

Key Words
Simultaneous heat and water transport, vadose zone, numerical simulation, climate change

Introduction
Prediction of effects of climate change on the vadose zone is a new application of numerical analysis of simultaneous heat and water movement between atmosphere and vadose zone. As well it is important since vadose zone is a foundation of ecosystem and agriculture. Changes in elements of climate such as air temperature, rainfall, and concentration of CO_2 would influence soil physical conditions such as moisture and temperature. Effects of climate change on soil have been discussed for many aspects. Nadden and Watts (2000) predicted the amount and distribution of available water resources in the United Kingdom with a fusion of Global Climate Model (GCM) and Land Surface Model (LSM) by focusing on the phenomena of soil surface and atmosphere. On the other hand, Huang (2006) showed soil temperature and downward heat flux in deep bore-holes all over the world has been rising for about 100 years. However, physical processes of water and heat transport in the vadose zone, and the boundary between atmosphere and soil related to climate change has not been discussed.

Though some models have already been proposed for simulating water and heat transport in the vadose zone, the models are not ready to simulate changes in heat and water conditions in response to future climate change such as temperature rise and variation of precipitation characteristics. One of the problems is a lack of comprehensive soil parameters and datasets corresponding to variety of climate and land use types for input and validation. For example, HYDRUS 1-D is a software system for simulating 1-dimensional heat, water and solute transport in unsaturated, partially and fully saturated porous media (Simunek *et al.* 2008). Its ver. 4.09 can consider surface energy balance as a boundary condition for bare soils (Saito *et al.* 2006). However, the model performance was mainly tested for dry regions and validation of energy balance was insufficient The purpose of this study is to test HYDRUS model performance for arable land in a monsoonal climate in order to predict impacts of future climate change on soil moisture and soil temperature in the vadose zone.

Methods
Field Monitoring
The field monitoring and soil sampling has been done at the Field Production Science Center in Graduate School of Agricultural and Life Sciences of the University of Tokyo (hereafter called Tanashi Farm) in Tanashi, Nishi-Tokyo City, western suburb of Tokyo (N 35°44′13″, E 139°32′30″). Monitoring period was from September 2008 to August 2009. The soil of 0 to 40cm under the surface was Kuroboku andisol, and below it to 100cm, Tachikawa loam andisol was distributed. A 10 m square area was prepared as the experimental site and kept bare through the experiment. There, albedo was observed using pyranometer (ML-020VL, EKO), and data of solar radiation, precipitation, air temperature, wind speed and relative humidity was obtained from weather station of Tanashi farm and AMeDAS (Automated Meteorological Data Acquisition System), belonging to Japan Meteorological Agency, near to the farm.

1 – 6 August 2010, Brisbane, Australia. Published on DVD.

Near the surface, heat flux plate (CHF-HFP01, Hukseflux Thermal Sensors) was laid for measuring soil surface heat flux. For monitoring soil moisture and soil temperature, TDR sensors (self-made) and copper-constantan thermocouples were inserted at depths of 3, 5, 7, 10, 20, 30, 50, 80cm. All sensors were connected to CR10X data logger (Campbell Sci.) and data was collected every 20 minutes for a year.

Determination of Soil Physical Properties

Water retention curves of the soils were measured in the laboratory by hanging water column method and pressure plate method. Then inverse analysis with evaporation method (Simunek *et al.* 1998) was applied to determine the soil hydraulic parameters for Durner Model (1984) [1].

$$S_e = \frac{\theta - \theta_r}{\theta_s - \theta_r} = w_1\left(1+\left|\alpha h\right|^{n_1}\right)^{-m_1} + w_2\left(1+\left|\alpha_2 h\right|^{n_2}\right)^{-m_2}$$

$$K(S_e) = K_s\left(w_1 S_{e1} + w_2 S_{e2}\right)^l \times \frac{\left(w_1\alpha\left[1-(1-S_{e1}^{1/m})^m\right] + w_2\alpha_2\left[1-(1-S_{e2}^{1/m2})^{m2}\right]\right)^2}{\left(w_1\alpha + w_2\alpha_2\right)} \quad [1]$$

where K_s is saturated hydraulic conductivity [m/s], S_e is effective saturation [-], and l, m=(1-1/n) and n are empirical parameters [-].Using the observed data of evaporation experiment, θ_r, θ_s, α, n, K_s, l ,w_2 , α_2 and n_2 in Durner model were estimated by inverse analysis by using HYDRUS 1-D.

Soil thermal conductivity λ at several different soil moisture contents was measured using KD2 heat probe (Decagon Devices) for both Kuroboku and Tachikawa loam. Then Chung and Horton (1987) model, eq. [2], was fitted to determine soil thermal parameters. Volumetric heat capacity of each sample was determined by weighed average corresponding to volumetric fraction of solid, air and water with eq. [3]

$$\lambda(\theta) = b_1 + b_2\theta + b_3\theta^{0.5} \quad [2]$$

$$C_p(\theta) = C_n\theta_n + C_o\theta_o + C_w\theta_w + C_a \approx 1.92\theta_n + 2.51\theta_o + 4.18\theta_w \quad [3]$$

where C is volumetric heat capacity, θ is volumetric fraction, n, o, w, and a show solid phase, organic matter, liquid water and air phase respectively.

Simulation of Water and Heat Transport in the Field

After determination of parameters, simulation of water and heat transport in vadose zone in the field from DOY1 (1st January, 2008) to DOY609 (31st August, 2009) was conducted by using HYDRUS. Depth of calculation profile was fixed as 100 cm, consisted of two layers according to field observation.

Boundary conditions for water and heat movement and input data needed for estimation are shown in Table 1. Because the exact initial soil moisture and thermal conditions and their sensitivity have not been known, preliminary calculation for preparing initial conditions was conducted. In the preliminary calculation, pressure head distribution of whole calculated profile -100cmH_2O, and temperature profile was after the observed data on December 31st, 2008. With these I.C.s , one year numerical simulation with B.C.s representing climate data of the experimental site had been done. Results of the preliminary calculation were employed as I.C.s for exact numerical simulation. Then model validation was done by comparing with the monitored and simulated values.

Table 1. Boundary Conditions and Input Data.

	Boundary	Condition	Input Data
Water	Upper	Precipitation intensity [cm/day]	Rainfall intensity
		Evaporation rate [cm/day]	Air temp. and R.H.
	Lower	Free drainage	
Heat	Upper	Surface heat flux [MJ m^2/day]	Solar radiation, air temp., wind speed, sunshine hour,
		Sensible heeat flux of precipitation [MJ m^2/day]	Rainfall intensity & Air temp.
	Lower	Zero gradient	

Results and Discussion

Fitting curves and measured soil water retention curves, unsaturated hydraulic conductivity and the relationship between volumetric water content and thermal conductivity for Kuroboku and Tachikawa loam are shown in Figure 1 from (a) to (c). Predicted solar radiation R_s and surface heat flux G were compared with observed ones as shown in Figure 2. Positive values indicate an incoming flux to the land surface (downward) while negative values imply outgoing flux from the land surface (upward). Both simulated surface heat flux and solar radiation described the dynamics of monitored values well. The meteorological model which employed HYDRUS is reasonable and proper for not only predicting soil surface radiation, but also producing thermal B.C. for soil surface.

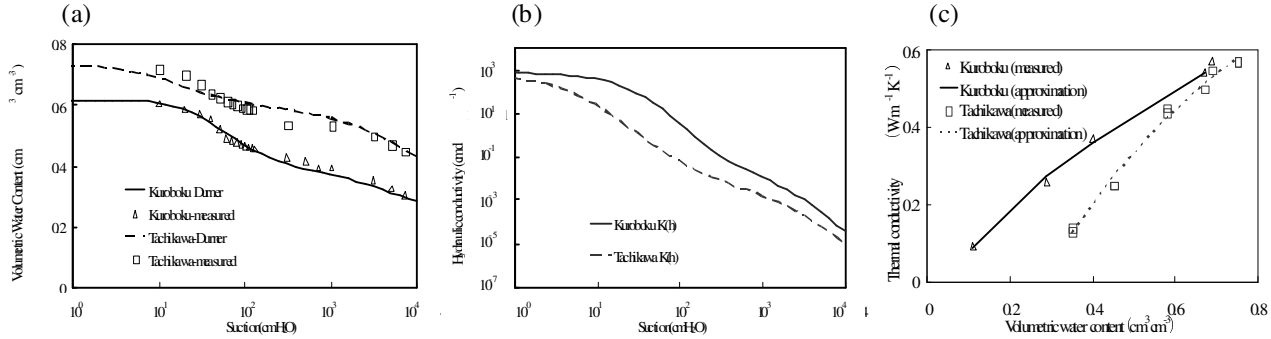

Figure 1. Simulated soil physical properties (a) water retention curves for Kuroboku and Tachikawa loam andisol, (b) unsaturated hydrolic conductivity (c) relation ship between soil moisture and soil thermal conductivity.

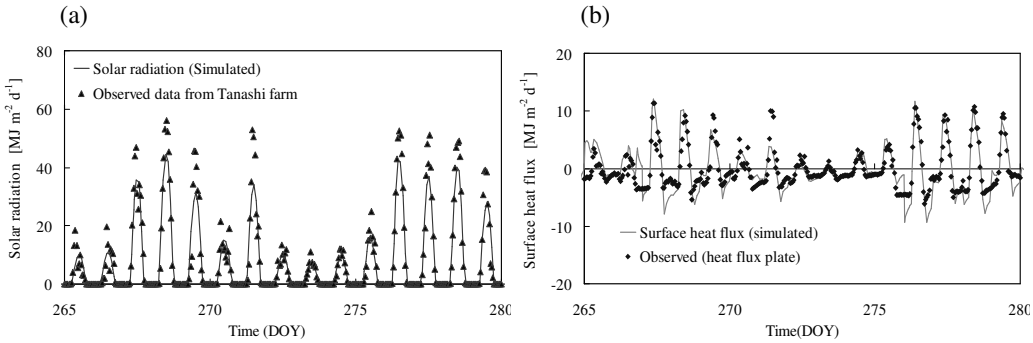

Figure 2. Validation of meteorological model (a) Surface heat flux (b) Solar radiation.

Figure 3 shows the soil temperature change at the depth of 3cm from (a) fall to winter, and (b) spring to summer. Simulated results described the observed temperature well especially in spring to summer. However, from fall to winter, simulated results tended to be underestimated soil temperature. It may be caused by lack of term describing latent heat and changes in heat capacity due to soil freezing in heat flow equation. Where soil frost is observed, it is better to consider the change in the amount of latent energy stored in the ice (Hansson *et al.* 2004)

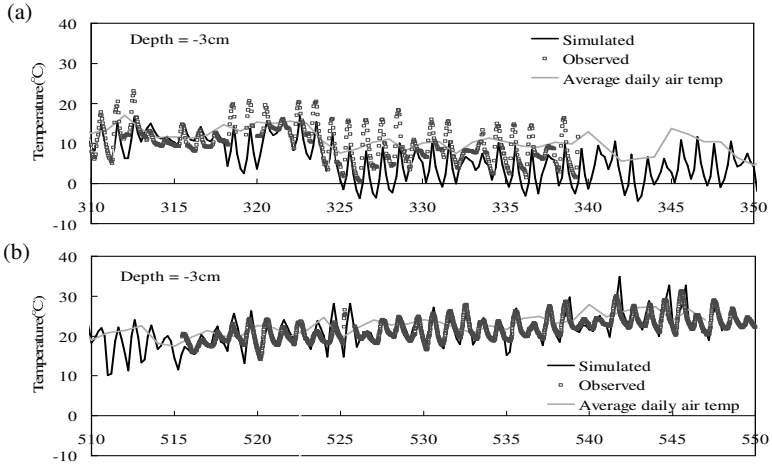

Figure 3. Comparison between simulated and observed soil temperature at the depth of 3cm (a) from DOY 250 (6th Sept., 2008) to DOY350 (15th Dec., 2008), (b) from DOY 510 (24th May, 2009) to DOY 550 (3rd July, 2009).

Figure 4 depicts daily rainfall record and simulated and measured soil moisture at four depths 7cm from DOY526 (9th June, 2009) to DOY609 (28th August, 2009). We could obtain the simulated soil moisture change reacting to the frequent rainfall and evaporation which is characteristic of the monsoon region. Recently, several kinds of GCM have been produced and improved in physical reliability and both spatial and temporal resolution. For example, some models provide predicted climate change in daily maximum, minimum and mean air temperatures, daily total precipitation, and daily accumulated shortwave radiation (Okada *et al.* 2009). Using these predicted climate data at such high temporal resolution, it will be possible to predict effects of climate change on soil physical condition in vadose zone with HYDRUS model as future work.

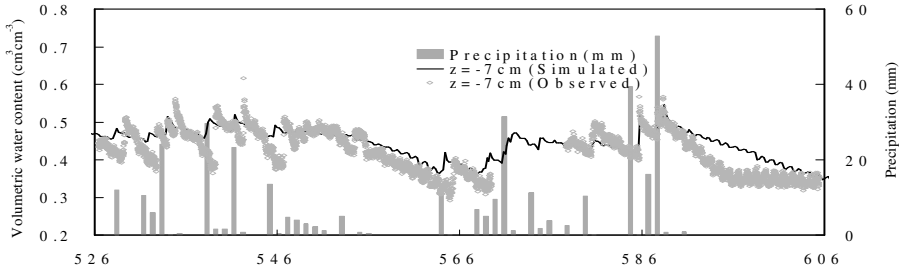

Figure 4. Comparison of predicted and observed soil temperature at the depth of 7cm from DOY 526 (9th June, 2009) to DOY609 (28th August, 2009).

Conclusions

We validated the model of simultaneous liquid water, vapor and heat transport across the border between atmosphere and vadose zone of arable land under a monsoonal climate with HYDRUS by comparing numerically simulated and observed values of surface energy balance, soil temperature and soil moisture. In calculation, soil hydraulic and thermal parameters were obtained by laboratory experiments and meteorological data being distributed to public had been used for input data for B.C.s. The simulation in general represented the monitored data well. So HYDRUS models could be considered to be proper and reasonable for the future use under monsoonal climate region. To improve the accuracy of the model, it would be necessary to consider the effect of soil freezing in winter.

References

Chung Horton (1987) Soil heat and water flow with a partial surface mulch. *Water Resour. Res.* **23,** 2175-2186

Durner W, (1994) Hydraulic Conductivity Estimation for Soils with Heterogeneous Pore Structure. *Water Resour. Res.* **30,** 211-223

Hansson K, J Simunek, M Mizoguchi, LC Lundin, MT van Genuchten. (2004) Water Flow and Heat Transport in Frozen Soil: Numerical Solution and Freeze-Thaw Applications. *Vadose Zone J.* **3,** 693-704

Huang S (2006) Land Warming as Part of Global Warming. *EOS (AGU)* **87**, 44.

IPCC (2007) Climate Change 2007. Synthesis Report. In 'Contribution of Working Groups I, II and III to the Fourth Assessment. Report of the Intergovernmental Panel on Climate Change' (Eds PK Pachauri, A Reisinger). (IPCC: Geneva, Switzerland, 104).

Naden PS, Watts CD (2001) Estimating climate-induced change in soil moisture at the landscape scale: an application to five areas of ecological interest in the U.K. *Clim. Change* **49,** 411-440

Okada M, Iizumi T, Nishimori M, Yokozawa M (2009) Mesh Climate Change Data of Japan Ver. 2 for Climate Change Impact Assessments Under IPCC SRES A1B and A2. *J. Agric. Meteorol* **65,** 97-109

Saito H, Simunek J, Mohanty BP (2006) Numerical analysis of Coupled Water, Vapor, and Heat Transport in the Vadose Zone. *Vadose Zone J*. **5,**784-800

Simunek J, Wendroth O, Th Van Genuchten M (1998) Parameter Estimation Analysis of the Evaporation Method for Determining Soil Hydraulic Properties. *Soil Sci. Soc. Am. J.* **62,** 894-905

Simunek J, Th Van Genuchten M, Sejna M (2008) Development and Applications of the HYDRUS and STANMOD Software Packages and Related Codes. *Vadose Zone J*. **7,** 587-600.

Comparison of regression pedotransfer functions and artificial neural networks for soil aggregate stability simulation

Adele Alijanpour shalmani[A], Mahmoud Shabanpour Shahrestani[B], Hossein Asadi[C] and Farid Bagheri [D]

[A] Msc. Student, University of Guilan, Rasht, Iran, Email adele.alijanpour@yahoo.com
[B]Faculty of Agriculture, University of Guilan, Rasht, Iran, Email m_shabanpur@yahoo.com
[C]Faculty of Agriculture, University of Guilan, Rasht, Iran, Email asadi@guilan.ac.ir
[D] Researcher, Tea Research center, Lahijan, Iran, Email faridbagheri@yahoo.com

Abstract
Simulation of soil aggregate stability is a suitable method for saving time and cost spent for direct measurement. This research comprises regression pedotransfer functions (RegPTFs) and artificial neural networks (ANNs) for estimation of soil aggregate stability. 140 soil samples from forest and rangland's soils of Guilan Province were collected and geometric mean diameter (GMD), %silt (Si), %clay (Cl), %sand (Sa), bulk density (BD), equivalent carbonate calcium ($CaCO_3$), particle density (PD), soil mechanical resistance (Load), pH, electrical conductivity (EC) and %organic matter (OM) values were determined. The data were split randomly into a calibration data subset (112 samples) and validation data subset (28 samples). Regression pedotransfer functions was performed by stepwise method and for establishing ANNs we used Marquardt-levenburg training algorithm and 3-layer perceptron structure with number of six neurons in one hidden layer. The best model of Regression functions for calibration GMD data was GMD=6.926-0.118pH-2.216PD-0.002Sa+0.103Load with R_{adj}^2=0.39. For determination of best ANNs model, we used five input patterns. Result showed that artificial neural networks with pH-PD-Sa-Load input pattern with R_{adj}^2= 0.87 for calibration GMD data, had most accurate prediction. With comparison of ANN with pH-PD-Sa-Load input pattern and regression pedotransfer functions, we found that ANNs with pH-PD-Sa-Load input pattern had higher R_{adj}^2 and Lower MSD (mean square of deviation) and hence ANNs could estimate soil aggregate stability better than regression pedotransfer functions.

Key Words
Simulation, soil aggregate stability, Pedotransfer function, artificial neural networks

Introduction
Soil aggregate stability determination is essential to erosion and conservation of soil, but direct measurement of Soil aggregate stability is time consuming and costly and so are called "Costly measured properties". However several researches have been done for indirect estimation of Soil aggregate stability from surrogate data such as texture, organic matter and bulk density. Regression pedotransfer functions and artificial neural networks are methods that can be used for simulation of Soil aggregate stability. Bouma (1989) expressed relationship between soil hydraulic properties and surrogate data such organic matter and bulk density and named it regression pedotransfer functions. Using regression pedotransfer function is not restricted to soil hydraulic properties estimation and used for simulation of soil chemical, biological and other physical properties. Artificial neural networks are intelligent modeling methods and can be used for costly measured soil properties estimation. They have the capability of learning complex relationship between multiple input and output variables (Nemes *et al*. 2002). Analysis of the ANN parameters suggested that more input variable and accurate data set were necessary to improve the prediction of costly measured soil properties (Tamari *et al*. 1996; Merdun *et al*. 2006).

Methods
In this research, 140 soil samples were collected from forest and rangland's soils of Guilan province. Soil samples were taken in each field at 0–20 cm depth for chemical and physical analyses. Then organic matter was determined by the Walkley and Black method, equivalent carbonate calcium was determined by titration method, pH was measured in suspension of soil to 0.01 M $CaCl_2$ ratio of 1:2.5 and electrical conductivity was measured in suspension of soil to water ratio of 1:5 (Page et al. 1982). Bulk density was determined by cylinder, particle density was determined by pycnometer, soil mechanical resistance was determined by penetrometer, fractions were used to measure particle size distributions (after complete dispersion with sodium hexametaphosphate) by the hydrometer method (klut. 1986) were determined as independent variables, and geometric mean diameter was determined by wet sieving apparatus (klut. 1986) was measured as dependent variable. The data were split randomly into a calibration data subset (112 samples) and validation data subset

(28 samples). Moreover, data subset used for determining the performance of two simulation method; artificial neural networks (ANNs) and regression pedotransfer functions (RegPTFs).
Estimation of soil aggregate stability using RegPTFs were initially carried out using SPSS 14 for windows with stepwise method.
For establishing ANNs, We used Neural Works plus software with marquardt-levenburg training algorithm and 3-layer perceptron structure with number of six neurons in hidden layer. The number of neurons in the input and output layers corresponded to the number of Input and output variables. The number of hidden layers and its neurons is determined by try and error method and assumed equal to 1 and 6 respectively. Activation function was defined as a sigmoid tangent function. The performance of the PTFs estimating the soil aggregate stability, were assessed using two criteria: coefficient's statistics of corrected explanation (R_{adj}^2), mean square of deviation (MSD).

Results

Regression equation for estimation of calibration GMD data are showed in Table 1. Our postulate was the best model has the lowest MSD and the highest R_{adj}^2. Descriptive statistics for GMD using five ANN models and regressions pedotransfer functions are summarized in Table 2. Graphs for best model ANN and same pattern in $RegPTF_s$ calibration data subset for GMD estimation with input independent data pH-PD-Sa-Load are showed in Figure 1. The R_{adj}^2 values of both five ANN models and regression pedotransfer functions were significant based on the analysis of variance (ANOVA test) ($P<0.01$). Generally, both ANN and regression models could predict GMD accurately but ANN performed slightly better. Artificial neural networks are better than regression models for simulation soil aggregate stability (Mohammadi. 2002).

Table 1. Regression equation for estimation of GMD of calibration data

input independent variables	regression equation
Load-Sa-$CaCO_3$	**GMD**=0.526+0.109**Load**-0.005**Sa**-0.016 **$CaCO_3$**
Sa-PD-$CaCO_3$	**GMD**=9.419-0.004**Sa**-2.946**PD**-0.026 **$CaCO_3$**
pH-PD-Sa-Load	**GMD**=6.926-0.118**pH**-2.216**PD**-0.002**Sa**+0.103**Load**
pH-PD-Sa	**GMD**=10.041-0.144**pH**-2.945**PD**-0.003**Sa**
pH-PD-Si	**GMD**=9.935-0.142**pH**-3.008**PD**+0.004**Si**

Table 2. Descriptive statistics for GMD using 16 ANN models and regressions pedotransfer functions

input independent variables	$R_{adj}^{2\ (cal)}$ ANN	MSD (cal) ANN	$R_{adj}^{2\ (cal)}$ RegPTFs	MSD (cal) RegPTFs	R_{adj}^2 (test) ANN	MSD (test) ANN
Load-Sa-$CaCO_3$	0.85	0.066	0.34	0.288	0.77	0.129
Sa-PD-$CaCO_3$	0.77	0.101	0.22	0.371	0.28	0.407
Ph-PD-Sa-Load	0.87	0.058	0.39	0.265	0.57	0.245
pH-PD-Sa	0.61	0.172	0.17	0.371	0.09	0.516
pH-PD-Si	0.83	0.073	0.20	0.372	0.37	0.345

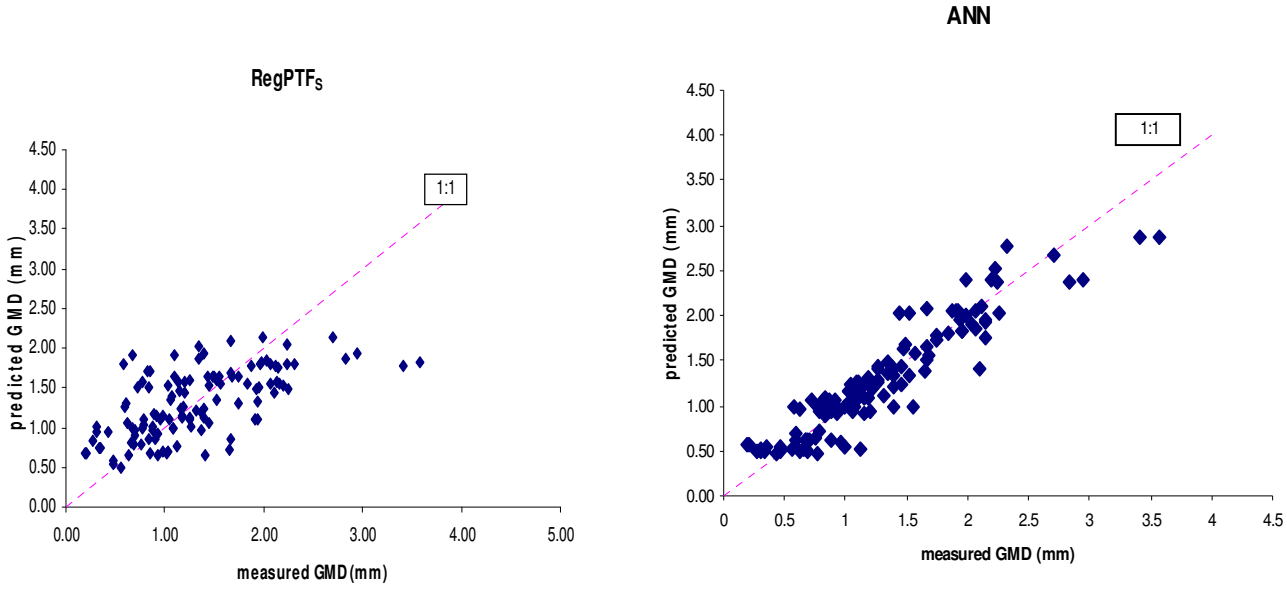

Figure 1. Graphs for best model ANN and similar pattern in RegPTF$_s$ calibration data subset for GMD estimation with input independent data (pH-PD-Sa-Load)

Conclusion

The best model of Regression functions for calibration GMD data was GMD=6.926-0.118pH-2.216PD-0.002Sa+0.103Load with R_{adj}^2=0.39 and MSD=0.265 for determination of best ANNs model, we used five input patterns. Result showed that artificial neural networks with pH-PD-Sa-Load input pattern with R_{adj}^2= 0.87 and MSD=0.058 for calibration GMD data, had most accurate prediction. With comparison of ANN with pH-PD-Sa-Load input pattern and regression pedotransfer functions, we found that ANNs with pH-PD-Sa-Load input pattern had higher R_{adj}^2 and Lower MSD (mean square of deviation) and hence ANNs could estimate soil aggregate stability better than RegPTF$_s$.

References

Bouma J (1989) Using soil survery data for quantitative land evaluation. *Soil Science Society of American Journal* **90**,177-213.

Klut A (1986) Method of Soil Analysis. Part 1.Physical and Mineralogical Properties. ASA, SSSA, Madison, Wisconsin, USA.

Merdun H, Cinar O, Meral R, Apan, M (2006) Comparioson of artificial neural network and regression pedotramsfer functions for prediction water retention and saturated hydraulic counductivity. *Soil & Tillage Res* **90**, 108-116.

Mohammadi J (2002) Testing an artificial neural network for predicting soil water retention characteristics from soil physical and chemical properties. 17 th WCSS. Thailand. Paper no:378. Paper no: 943.

Nemes A, Pachepsky Y, Rawls W, Wosten H, Zeilguer, A (2002) Using similarity and neural network approach to inter plate soil particle- size distribution. 17 th WCSS. Thailand. Paper No: 221. Paper No: 943.

Page AL, Miller RH, Keeney, DR (1982) Method of Soil Analysis. Part 2. Chemical and Microbiological Properties. ASA, SSSA, Madison, Wisconsin, USA.

Tamari S, Wosten JHM, Ruiz-Suarez, JC (1996) Testing an artificial neural network for predicting soil hydraulic conductivity. *Soil Science Society of American Journal* **60**, 1732-1741.

Comparison of the results of modelling soil loss with WEPP and USLE in the Koppány Valley, Hungary

Géza Gelencsér[A], Csaba Centeri[A], Gergely Jakab[B], Márton Vona[C]

[A]Department of Nature Conservation and Landscape Ecology, Institute of Environmental and Landscape Management, Faculty of Agricultural and Environmental Sciences, Szent István University, 2103-Gödöllő, Páter K. u. 1., Hungary, Email Centeri.Csaba@kti.szie.hu
[B]Research Institute of Geography, Hungarian Academy of Sciences, H-1112-Budapest, XI. Budaörsi ut 45., Hungary, Email jakab@sparc.core.hu
[C]Central Authority of Water and Environment, 1012 Budapest, Márvány u. 1/d, D/108. sz.

Abstract
Soil water erosion prediction is the backbone of outlining hot spots where soil and nutrient loss might reach the biggest proportion, causing yield loss thus deficit for the farmer; sedimentation on the farm – deficit again –; siltation (filling up) and pollution of waterways and lakes putting the task of cleaning the roadside on the shoulder of local communities etc. It is important to find the best solution, the most appropriate, close to natural reality calculation or modelling of soil and nutrient loss and runoff. In the present study WEPP and USLE model were used to prove their efficiency on a slope of intensive arable farmland, close to the Koppány Creek. Along the creek we can find a NATURA 2000 site so it is not only important for the sake of the clean water itself but there are high natural values to be considered. The results show that on the upper and middle slope sections WEPP calculates more soil loss than USLE while at the bottom of the slopes WEPP calculates much more than USLE. On site investigations proved that the lower part of the slope is sedimented so USLE is closer to reality at the bottom of the slope.

Key Words
Soil water erosion, modelling, soil loss, WEPP, USLE, natural values.

Introduction
Soil erosion is a serious problem on agricultural fields of Hungary. In the hilly areas precipitation is between 600 and 800 mm/year. Even the relatively low intensity rainfalls are causing gullying and rills. The crop rotation structure does not favour soil protection, contains a high percentage of medium or low soil protection crop (Centeri 2002, Szilassi *et al*. 2006). Soil and nutrient loss, runoff and sediment yield calculations (Jakab and Szalai 2005) are important in protecting our (still) valuable arable lands. Examination of soil parameters are essential to teach farmers for better management practices in order to save nutrients, soils, money, time and to protect the environment (Jordan *et al.* 2005). Soil and nutrient loss are calculated in erosion models all over the world (Gournellos *et al*. 2004), especially in connection with arable cultivation. The area suffers "rural exodus", all the young people have already left the region thus land use can be characterized by intensive farming on the areas of the former cooperative and quasi extensive use on the other part of the area thanks to the lack of local workers.

Methods
The well-known USLE (Wischmeier and Smith 1978) and WEPP (Flanagan *et al.* 2007) models were used for the analyses. The Water Erosion Prediction Project (WEPP) was started in 1985. Its purpose was to develop new-generation water erosion prediction technology, originally (as well as the USLE) for use in the USA. The WEPP model was developed by the USDA-ARS to replace empirically based erosion prediction technologies, such as USLE, RUSLE, MUSLE. The WEPP model simulates many of the formerly missing physical processes important in soil erosion (e.g. infiltration, runoff, raindrop and flow detachment, sediment transport, deposition, plant growth, and residue decomposition) as input parameters. The WEPP project is similar to USLE because it was constructed based on extensive field experimental program (on cropland, rangeland and disturbed forest sites). Sufficient amount of data was needed to parameterize and test the model. The model became functional with the cooperation of research locations, laboratories and universities. The WEPP model can be used on hill slopes and on smaller watersheds. The model can be used with Microsoft Windows operating system graphical interfaces, web-based interfaces, and integration with Geographic Information Systems since 1995. Watershed channel and impoundment components, CLIGEN weather generator, the daily water balance and evapotranspiration routines, and the prediction of subsurface lateral flow along low-permeability soil layers was developed and continuously improved (Chaves and Nearing 1991; Risse *et al*. 1994; Flanagan *et al*. 2007; Deer-

Ascough *et al*. 1995; Grismer 2007; Moffet *et al*. 2007; Kim *et al*. 2007; Bonilla *et al*. 2007; Moore *et al*. 2007).

WEPP is widely used for soil loss calculations (Pandey *et al*. 2008, Shen *et al*. 2009, Irvem *et al*. 2007, Baigorria and Romero 2007).

Input parameters for the WEPP model: rainfall (amount 16.50 mm, duration 48 min), normalized peak intensity (2.73), normalized time to peak (0.15). Land use was tilled fallow. Slope length and slope angle was calculated based on the topography map of the area and on in situ check with GPS. Input parameters for the USLE model were: R = E = 0.06934, K = 0.009, LS = 4.75 (slope length was 240m (first section's plane length was 44.16m, second section's plane length was 157.98m, third section's plane length was 37.85m; slope length was 8, 6 and 4%), C = 1 (for black fallow), P=1.

Results

The results of soil loss calculations with USLE model can be found in Table 1.

Table 1. Input parameters and results of the simulation with the USLE model, Gerézdpuszta, Hungary

Slope section	R factor*	K factor	L factor	S factor	Soil loss (kg/m^2)
Upper	0.06934	0.38	1.42	0.85	0.543496
Middle		0.009	1.83	0.57	0.011124
Lower		0.0001	1.31	0.35	0.000054

**in this special case, since the calculation is for one rainfall event, this is erosivity index, C and P factors = 1*

The results of soil loss calculations with WEPP model can be found in Tables 2-4.

Table 2. Results of the simulation with the WEPP model for the upper slope third, Gerézdpuszta, Hungary

PD (m)	**SOL**	**PD (m)**	**SOL**	**PD (m)**	**SOL**	**PD (m)**	**SOL**	**PD (m)**	**SOL**
(m)	(kg/m^2)	**(m)**	(kg/m^2)	**(m)**	(kg/m^2)	**(m)**	(kg/m^2)	**(m)**	(kg/m^2)
0.44	0.014	9.27	0.016	18.11	0.447	26.94	0.683	35.77	0.864
0.88	0.014	9.72	0.042	18.55	0.461	27.38	0.693	36.21	0.872
1.32	0.014	10.16	0.076	18.99	0.474	27.82	0.703	36.65	0.880
1.77	0.014	10.60	0.111	19.43	0.487	28.26	0.713	37.10	0.888
2.21	0.014	11.04	0.146	19.87	0.500	28.71	0.723	37.54	0.895
2.65	0.014	11.48	0.181	20.31	0.513	29.15	0.733	37.98	0.903
3.09	0.014	11.92	0.217	20.76	0.525	29.59	0.742	38.42	0.910
3.53	0.014	12.37	0.246	21.20	0.538	30.03	0.752	38.86	0.918
3.97	0.014	12.81	0.264	21.64	0.550	30.47	0.761	39.30	0.925
4.42	0.014	13.25	0.281	22.08	0.562	30.91	0.770	39.75	0.933
4.86	0.014	13.69	0.297	22.52	0.574	31.36	0.779	40.19	0.940
5.30	0.014	14.13	0.313	22.96	0.585	31.80	0.788	40.63	0.947
5.74	0.014	14.57	0.329	23.41	0.597	32.24	0.797	41.07	0.954
6.18	0.014	15.02	0.345	23.85	0.608	32.68	0.806	41.51	0.961
6.62	0.014	15.46	0.360	24.29	0.619	33.12	0.814	41.95	0.968
7.07	0.014	15.90	0.375	24.73	0.630	33.56	0.823	42.40	0.975
7.51	0.014	16.34	0.390	25.17	0.641	34.00	0.831	42.84	0.982
7.95	0.014	16.78	0.405	25.61	0.652	34.45	0.840	43.28	0.988
8.39	0.014	17.22	0.419	26.06	0.662	34.89	0.848	43.72	0.995
8.83	0.014	17.66	0.433	26.50	0.673	35.33	0.856	44.16	1.002

PD = Profile distances are from top to bottom of hillslope, SOL = Soil loss

Table 3. Results of the simulation with the WEPP model for the middle slope third, Gerézdpuszta, Hungary

PD (m)	SOL	PD (m)	SOL	PD (m)	SOL	PD (m)	SOL	PD (m)	SOL
(m)	(kg/m^2)	(m)	(kg/m^2)	(m)	(kg/m^2)	(m)	(kg/m^2)	(m)	(kg/m^2)
45.74	0.419	77.34	0.520	108.94	0.609	140.53	0.626	172.13	0.696
47.32	0.424	78.92	0.525	110.52	0.608	142.11	0.630	173.71	0.699
48.90	0.430	80.50	0.529	112.10	0.608	143.69	0.633	175.29	0.702
50.48	0.435	82.08	0.534	113.68	0.607	145.27	0.637	176.87	0.706
52.06	0.440	83.66	0.539	115.26	0.606	146.85	0.641	178.45	0.709
53.64	0.445	85.24	0.543	116.84	0.605	148.43	0.644	180.03	0.714
55.22	0.451	86.82	0.548	118.41	0.603	150.01	0.648	181.61	0.736
56.80	0.456	88.40	0.552	119.99	0.602	151.59	0.651	183.19	0.762
58.38	0.461	89.98	0.557	121.57	0.601	153.17	0.655	184.77	0.787
59.96	0.466	91.56	0.561	123.15	0.599	154.75	0.658	186.35	0.813
61.54	0.471	93.14	0.566	124.73	0.598	156.33	0.662	187.93	0.839
63.12	0.476	94.72	0.570	126.31	0.596	157.91	0.665	189.51	0.864
64.70	0.481	96.30	0.575	127.89	0.597	159.49	0.669	191.09	0.890
66.28	0.486	97.88	0.579	129.47	0.600	161.07	0.672	192.67	0.908
67.86	0.491	99.46	0.584	131.05	0.604	162.65	0.675	194.25	0.912
69.44	0.496	101.04	0.588	132.63	0.608	164.23	0.679	195.83	0.916
71.02	0.501	102.62	0.592	134.21	0.611	165.81	0.682	197.41	0.919
72.60	0.506	104.20	0.597	135.79	0.615	167.39	0.686	198.99	0.923
74.18	0.510	105.78	0.601	137.37	0.619	168.97	0.689	200.57	0.926
75.76	0.515	107.36	0.605	138.95	0.622	170.55	0.692	202.15	0.930

PD = Profile distances are from top to bottom of hillslope, SOL = Soil loss

Table 4. Results of the simulation with the WEPP model for the lower slope third, Gerézdpuszta, Hungary

PD (m)	SOL	PD (m)	SOL	PD (m)	SOL	PD (m)	SOL	PD (m)	SOL
(m)	(kg/m^2)	(m)	(kg/m^2)	(m)	(kg/m^2)	(m)	(kg/m^2)	(m)	(kg/m^2)
202.53	1.191	210.10	1.184	217.67	1.176	225.24	1.169	232.81	1.161
202.90	1.191	210.47	1.183	218.05	1.176	225.62	1.168	233.19	1.161
203.28	1.191	210.85	1.183	218.42	1.175	225.99	1.168	233.56	1.160
203.66	1.190	211.23	1.183	218.80	1.175	226.37	1.168	233.94	1.160
204.04	1.190	211.61	1.182	219.18	1.175	226.75	1.167	234.32	1.160
204.42	1.189	211.99	1.182	219.56	1.174	227.13	1.167	234.70	1.158
204.80	1.189	212.37	1.181	219.94	1.174	227.51	1.166	235.08	1.127
205.18	1.189	212.75	1.181	220.32	1.173	227.89	1.166	235.46	1.083
205.55	1.188	213.12	1.181	220.69	1.173	228.27	1.166	235.84	1.040
205.93	1.188	213.50	1.180	221.07	1.173	228.64	1.165	236.21	0.995
206.31	1.187	213.88	1.180	221.45	1.172	229.02	1.165	236.59	0.951
206.69	1.187	214.26	1.180	221.83	1.172	229.40	1.165	236.97	0.905
207.07	1.187	214.64	1.179	222.21	1.172	229.78	1.164	237.35	0.859
207.45	1.186	215.02	1.179	222.59	1.171	230.16	1.164	237.73	0.812
207.82	1.186	215.40	1.178	222.97	1.171	230.54	1.163	238.11	0.764
208.20	1.186	215.77	1.178	223.34	1.170	230.92	1.163	238.49	0.716
208.58	1.185	216.15	1.178	223.72	1.170	231.29	1.163	238.86	0.667
208.96	1.185	216.53	1.177	224.10	1.170	231.67	1.162	239.24	0.617
209.34	1.184	216.91	1.177	224.48	1.169	232.05	1.162	239.62	0.566
209.72	1.184	217.29	1.176	224.86	1.169	232.43	1.162	240.00	0.514

PD = Profile distances are from top to bottom of hillslope, SOL = Soil loss

Tables 2-4. show that a not too big rainfall event, arriving on the area with bad timing (no surface cover) can cause 10 t ha^{-1} soil loss.

Conclusion

It has always been emphasized that local measurements have very high importance so we do not wish to conclude this well-known fact again but we would like to call attention on carefully choosing the input parameters. In the present case a very simple method proved that the high amount of calculated soil loss is not proper since parent material was found at the depth of 180-200cm below surface.

On the other hand, it is important information for local farmers that a relatively small (45mm h^{-1}) intensity precipitation can cause very high amount of soil loss. The only way to protect the land against it is to have some

soil loss measure, plant residues on the surface, another crop or some technical improvements.
Furthermore detailed local knowledge from the soils can save energy, fertilizer, time and money for the farmers.

References

Baigorria GA, Romero CC (2007) Assessment of erosion hotspots in a watershed: integrating the WEPP model and GIS in a case study in the Peruvian Andes. *Environ. Modell. Softw.* **22**(8), 1175–1183.

Bonilla CA, Norman JA, Molling CC (2007) Water erosion estimation in topographically complex landscapes: Model description and first verifications. *Soil Science Society of America Journal* **71(**5**),** 1524–1537**.**

Centeri Cs (2002) The role of vegetation cover in soil erosion on the Tihany Peninsula. *Acta Botanica Hungarica* **44**(3-4), 285–295.

Chaves HML, Nearing MA (1991) Uncertainty analysis of the WEPP soil erosion model. *Transactions of the ASAE* **34**, 2437–2444.

Deer-Ascough LA, Weesies GA, Ascough II JC, Laflen JM (1995) Plant parameter database for erosion prediction models. *Applied Engineering in Agriculture of ASAE* **11**(5), 659–666.

Flanagan DC, Gilley JE, Franti TG (2007) Water Erosion Prediction Project (WEPP): Development history, model capabilities, and future enhancements. *Transactions of the ASABE* **50**(5), 1603–1612.

Gournellos Th, Evelpidou N, Vassilopoulos A (2004) Developing an Erosion risk map using soft computing methods (case study at Sifnos island). *Natural Hazards* **31**(1), 39–61.

Grismer ME (2007) Soil restoration and erosion control: Quantitative assessment and direction. *Transactions of the ASABE* **50**(5), 1619–1626.

Irvem A, Topaloğlu F, Uygur V (2007) Estimating spatial distribution of soil loss over Seyhan River Basin in Turkey. *Journal of Hydrology* **336**, 30–37.

Jakab G, Szalai Z (2005) Erodibility measurements in the Tetves catchment using rainfall simulator. Tájökológiai Lapok. *Hungarian Journal of Landscape Ecology* **3**(1), 177–189. (in Hungarian)

Jordan Gy, van Rompaey A, Szilassi P, Csillag G, Mannaerts C, Woldai T (2005) Historical land use changes and their impact on sediment fluxes in the Balaton basin (Hungary). *Agriculture, Ecosystems and Environment* **108**, 119–130.

Kim IJ, Hutchinson SL, Hutchinson JMS, Young CB (2007) Riparian ecosystem management model: Sensitivity to soil, vegetation, and weather input parameters. *Journal of the American Water Resources Association* **43**(5), 1171–1182.

Moffet CA, Pierson FB, Robichaud PR, Spaeth KE, Hardegree SP (2007) Modeling soil erosion on steep sagebrush rangeland before and after prescribed fire. *Catena* **71**(2), 218–228.

Pandey A, Chowday VM, Mal BC, Billib M (2008) Runoff and sediment yield modeling from a small agricultural watershed in India using the WEPP model. *Journal of Hydrology* **348**, 305–319.

Risse LM, Nearing MA, Savabi MR (1994) Determining the Green and Ampt effective hydraulic conductivity from rainfall-runoff data for the WEPP model. *Transactions of the ASAE* **37**, 411–418.

Shen ZY, Gong YW, Li YH, Hong Q, Xu L, Liu RM (2009) A comparison of WEPP and SWAT for modeling soil erosion of the Zhangjiachong Watershed in the Three Gorges Reservoir Area. *Agricultural Water Management*, **96**, 1435–1442.

Szilassi P, Jordan G, van Rompaey A, Csillag G (2006) Impacts of historical land use changes on erosion and agricultural soil properties in the Kali Basin at Lake Balaton, Hungary. *Catena* **68**(3), 96–108.

Wischmeier WH, Smith DD (1978) Predicting rainfall erosion losses: A guide to conservation planning. U.S. Department of Agriculture. Handbook no. 537.

DEM and terrain analysis to predict spatial pattern of SOC

Beng Umali[A], David Chittleborough[A], Rai Kookana[B] and Bertram Ostendorf[A]

[A]School of Earth and Environmental Sciences, University of Adelaide, Urrbrae, SA, Australia, Email beng.umali@adelaide.edu.au
[B]CSIRO Land and Water, Urrbrae, SA, Australia.

Abstract
A simple approach to predict spatial pattern of SOC using a surrogate variable, soil Munsell value, with the aid of digital terrain analysis is presented. Digital elevation models (DEMs) were prepared using readily available digital topographic maps and then enhanced for a small sloping catchment in the Adelaide hills using plausibility algorithms. Seven terrain parameters were calculated from the DEMs. One hundred random points were identified across the 5.6 ha site and soil Munsell value was obtained. Correlation analysis showed elevation, specific catchment area, profile curvature, and wetness index influence soil Munsell value. It was also found that the application of plausibility algorithms to DEMs derived from topographic maps produced better correlation coefficients compared to unsmooth DEMs.

Key Words
Soil Munsell value, digital terrain parameters.

Introduction

Soil organic carbon (SOC) influences crop yield and acts as binding material for nutrients and agrochemicals (Konen *et al.* 2003; Lal 2007). Quantifying and mapping the spatial distribution of SOC is therefore important to an effective farm management as well as in broad carbon cycle modelling (Wills *et al.* 2007). Accurate but practical means of elucidating spatial distribution of SOC is needed because current laboratory quantification is overwhelmingly expensive. Soil colour, particularly Munsell value, has been used as a surrogate for SOC (Konen *et al.* 2003; Schulze *et al.* 1993; Wills *et al.* 2007) where darker soils are associated with high SOC and lighter soils with low SOC. Although soil colour determination using Munsell Colour Chart is subjective, it can be used to assess the distribution of SOC across large landscapes (Wills *et al.* 2007). SOC pattern in the landscape is also strongly influenced by the distribution of water and soil material (Pennock and Corre 2001) such that it can be predicted from terrain. Terrain parameters can be readily derived from digital elevation models (DEM) and particularly those relating to water flow accumulation and dissipation are well suited to predict SOC and soil colour (Gessler *et al.* 1995; Moore *et al.* 1991). However, SOC distribution is site specific and fundamentally affected by agronomic management. The utility of soil colour measurement and terrain analysis, which are both easy and intuitive, to infer spatial distribution of SOC in an agronomically homogenous landscape has not been fully explored. Thus, this research was conducted if terrain attributes calculated from topographic maps can be used to infer spatial distribution of SOC through soil colour in a hilly apple tree orchard. This research also investigated the effect of plausibility algorithms in preparing hydrologically correct DEM.

Methods

A sloping area located within the Mt. Lofty Ranges (30 km east of Adelaide, South Australia) has been selected for this purpose (Figure 1). The subcatchment has a relief of about 100 m and a Mediterranean climate. The site has brown duplex soil overlying a Stonyfell Quartzite formation (Heath 1963). The apple orchard was established in the early 1950s and little soil trenching was done prior to tree establishment. Topographic maps (1:10,000 and 1:50,000) in digital format have been sourced from the Department of Environment and Heritage – South Australia. Both maps were derived from analogue photogrammetric techniques and scanned then converted to GIS formats. The 1:10,000 map has a contour interval of 5 m. The 1:50,000 map has a contour interval of 10 m. Both maps have unknown vertical and horizontal accuracy.
A 5x5 m and a 10x10 m pixel DEM were generated for each of the two topographic data using the Topo to Raster tool in ArcGIS 9.2 incorporating drainage enforcement and sink filling. One of the main problems in soil-terrain modelling is the accuracy of available topographic data suitable for regional soil mapping. This can addressed through plausibility algorithms that reduces errors in DEM generation (Hengl *et al.* 2004).Two plausibility algorithms were then carried out to enhance the quality of the DEMs. The first algorithm involved the reduction of outliers through low pass filtering. The second one involved the reduction of padi terraces using focal mean statistics. Both algorithms were done on a 3x3 moving window. This resulted to four (4) DEMs

namely: s5-5; s5-10; s10-5; and s10-10. These DEMs where then compared with the interpolated 5x5 m pixel DEM of the 1:10,000 topographic map and 10x10m pixel DEM of the 1:50,000 topographic map (hereinafter referred as r5 and r10, respectively). Seven (7) key terrain parameters (Table 1) were calculated in GIS environment for each of the DEM using a freely available software called Terrain Analysis System (Lindsay 2006) and the distributional algorithm developed by Ostendorf and Reynolds (1993).

One hundred locations were randomly selected across a 5.6 ha area within the subcatchment. Points were referenced on the ground using a handheld high-sensitivity GPS. Each point consisted of 5 soil samples 0.5 m apart in a Z configuration. The top 10 cm of soil found between apple tree rows was obtained with a soil auger. Soil samples were air-dried, composited and analysed in the laboratory. Air-dry soil colour was determined using Munsell® Colour Chart (1998 edition) under natural diffuse daylight. Soil Munsell value was extracted and tabulated against the aforementioned topographic parameters including elevation obtained by nearest neighbourhood sampling of the DEMs. Spearman rank correlation analysis was performed to determine the degree of relationship and to compare the various DEM qualities and resolutions.

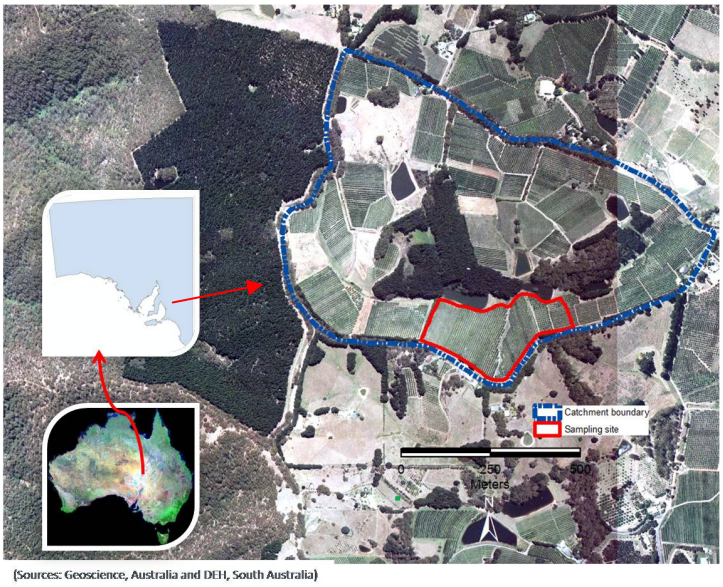

Figure 1. Location of the study site.

Table 1. Terrain parameters calculated in this study.

Attribute	Description
Slope,	
Plan curvature (PlanC), /m	a measure of topographic convergence and divergence
Profile curvature (ProfC), /m	a measure of flow acceleration or deceleration
Tangential curvature (TanC), /m	a measure of flow convergence and divergence
Specific catchment area (SCA), m^2/m	the ratio of the area upslope of a contour segment that contributes flow to that segment and the length of that segment
Sediment transport capacity index (STCI)	equivalent to RUSLE Length-Slope factor
Wetness index (WI)	the ratio of specific catchment area and slope

Results

The resulting DEM varied across the various pixel qualities and resolutions prepared as evidenced by the differing statistical measures of terrain parameters (Table 2). Slope and curvature parameters, for instance, became subtler after two smoothing operations (low pass filtering and focal mean statistics) were done on both topographic map scales. Moreover, increasing the pixel size resulted to a more generalised topography. Thompson et al (2001) attributed this to loss of details as a result of smoothing the topography.

Spearman rank correlation analysis reveals elevation, ProfC, SCA and WI correlates well with soil Munsell value (Table 3) in the study site. These observations were congruent to those of Gessler *et al* (2000), Moore *et al* (1993), Takata *et al* (2007), and Thompson *et al* (Thompson *et al.* 2001). The directions of correlation were similar for all DEMs prepared. However, the magnitude and significance varied depending on the quality of the DEM. A smoother DEM improved the correlation regardless pixel size.

Table 2. Summary statistics of terrain parameters across the different DEM resolution and quality.

Terrain parameters	Statistics	DEM					
		r5	s5-5	s5-10	r10	s10-5	s10-10
Slope	min	6.08	6.81	6.70	2.80	3.38	1.96
	μ	13.2	12.9	11.9	12.4	12.3	11.17
	max	20.9	19.2	16.9	21.6	20.3	18.1
	S	2.99	2.62	2.41	3.90	3.76	3.21
Plan curvature	min	-3.92	-3.27	-2.10	-3.02	-3.54	-3.42
	μ	-0.179	0.166	0.0460	-0.059	0.0715	-0.0258
	max	4.19	1.88	1.23	3.68	2.24	1.20
	S	1.11	0.86	0.611	1.16	0.915	0.738
Profile curvature	min	-0.909	-0.359	-0.268	-0.700	-0.387	-0.238
	μ	-0.0079	-0.00766	-0.0181	0.00617	0.0167	0.00854
	max	0.733	0.599	0.323	0.882	0.453	0.308
	S	0.260	0.159	0.117	0.230	0.213	0.136
Tangential curvature	min	-0.709	-0.374	-0.213	-0.499	-0.333	-0.214
	μ	-0.0302	-0.0344	-0.0157	-0.0143	-0.0177	-0.00743
	max	0.781	0.421	0.279	0.658	0.671	0.307
	S	0.222	0.159	0.104	0.206	0.174	0.109
Specific catchment area	min	9.99	5.08	10.0	18.5	5.11	10.0
	μ	58.3	54.1	76.2	84.6	76.5	78.4
	max	392.	770	480	1680.	1370	570
	S	56.5	79.3	81.2	170.	168	88.6
Sediment transport capacity index	min	0.999	0.589	1.56	0.750	0.771	1.19
	μ	5.71	5.15	5.49	5.89	5.33	4.99
	max	18.6	21.9	14.5	14.3	31.5	13.2
	S	3.02	3.09	2.53	2.83	4.35	2.43
Wetness index	min	3.82	2.94	3.51	4.22	2.99	3.97
	μ	5.28	5.12	5.59	5.62	5.29	5.66
	max	7.69	8.30	7.95	10.4	9.71	9.72
	S	0.67	0.824	0.846	0.849	1.06	0.987

Min– minimum; max – maximum; μ – mean; S – standard deviation; r5 – interpolated 5m pixel DEM from 1:10,000 map; r10 – interpolated 10m pixel DEM from 1:50,000 map; s5-5 – smooth 5m pixel DEM from 1:10,000 map; s5-10 – smooth 10m pixel DEM from 1:10,000 map; s10-5 – smooth 5m pixel DEM from 1:50,000 map; s10-10 – smooth 10m pixel DEM from 1:50,000 map

Table 3. Comparison of DEM using Spearman's rank correlation of Munsell value and terrain parameters.

Parameters	DEM					
	R5	S0505	S0510	R10	S1005	S1010
Elevation	0.488 ***	0.494 ***	0.488 ***	0.492 ***	0.487 ***	0.48 ***
Slope	0.014 ns	0.032 ns	0.025 ns	0.12 ns	0.108 ns	0.123 ns
PlanC	-0.089 ns	-0.196 *	-0.24 *	-0.075 ns	-0.102 ns	-0.147 ns
ProfC	-0.152 ns	-0.267 **	-0.35 ***	-0.261 **	-0.235 *	-0.364 ***
TanC	-0.102 ns	-0.204 *	-0.25 *	-0.078 ns	-0.061 ns	-0.116 ns
SCA	-0.354 ***	-0.432 ***	-0.402 ***	-0.287 **	-0.358 ***	-0.353 ***
STCI	-0.222 *	-0.273 **	-0.314 ***	-0.108 ns	-0.124 ns	-0.107 ns
WI	-0.39 ***	-0.466 ***	-0.407 ***	-0.224 *	-0.308 **	-0.357 ***

Please see DEM notation on Table 2; * α = 0.05; ** α = 0.01; *** α = 0.001; ns – not significant

Conclusion

Various digital terrain models have been derived from existing topographic data (available from state mapping agencies; derived from early topographic surveys) and provided valuable tool in soil-landscape modeling. Smoothing the DEM enhanced terrain models.

References

Akaike H (1974) New look at the statistical model identification. *IEEE Transactions on Automatic Control* **AC-19,** 716-723.

Gessler PE, Chadwick OA, Chamran F, Althouse L, Holmes K (2000) Modeling soil-landscape and ecosystem properties using terrain attributes. *Soil Science Society of America Journal* **64,** 2046-2056.

Gessler PE, Moore ID, McKenzie NJ, Ryan PJ (1995) Soil-landscape modelling and spatial prediction of soil attributes. *International Journal of Geographical Information Systems* **9,** 421-432.

Heath GR (1963) Stonyfell quartzite: Descriptive stratigraphy and petrography of the type section. *Trans. Roy. Soc. S. Aust.* **87,** 159-166.

Hengl T, Gruber S, Shrestha DP (2004) Reduction of errors in digital terrain parameters used in soil-landscape modelling. *International Journal of Applied Earth Observation and Geoinformation* **5,** 97-112.

Jenny H (1941) 'Factors of soil formation: a system of quantitative pedology.' (Mcgraw-hill: N.Y).

Konen ME, Burras CL, Sandor JA (2003) Organic Carbon, Texture, and Quantitative Color Measurement Relationships for Cultivated Soils in North Central Iowa. *Soil Science Society of America Journal* **67,** 1823-1830.

Lal R (2007) Farming carbon. *Soil and Tillage Research* **96,** 1-5.

Lindsay J (2006) 'Terrain Analysis System'.

Moore ID, Gessler PE, Nielsen GA, Peterson GA (1993) Soil attribute prediction using terrain analysis. *Soil Science Society of America Journal* **57,** 443-452.

Moore ID, Grayson RB, Ladson AR (1991) Digital terrain modeling - a review of hydrological, geomorphological and biological applications. *Hydrological Processes* **5,** 3-30.

Ostendorf BF, Reynolds JF (1993) Relationships between a terrain-based hydrologic model and patch-scale vegetation patter in an arctic tundra landscape. *Landscape Ecology* **8,** 229-237.

Pennock DJ, Corre MD (2001) Development and application of landform segmentation procedures. *Soil and Tillage Research* **58,** 151-162.

Schulze DG, Nagel JL, Van Scoyoc GE, Henderson TL, Baumgardner MF, Stott DE (1993) Significance of organic matter in determining soil colors. *Soil color. Proc. symposium, San Antonio **1990**,* 71-90.

Takata Y, Funakawa S, Akshalov K, Ishida N, Kosaki T (2007) Spatial prediction of soil organic matter in northern Kazakhstan based on topographic and vegetation information. *Soil Science and Plant Nutrition* **53,** 289-299.

Thompson JA, Bell JC, Butler CA (2001) Digital elevation model resolution: Effects on terrain attribute calculation and quantitative soil-landscape modeling. *Geoderma* **100,** 67-89.

Wills SA, Burras CL, Sandor JA (2007) Prediction of soil organic carbon content using field and laboratory measurements of soil color. *Soil Science Society of America Journal* **71,** 380-388.

Digital soil-landscape mapping by image clustering

Daniel Brough[A,B] and Robin Thwaites[B]

[A]Department of Environment and Resource Management, Indooroopilly, QLD, Australia, Email daniel.brough@derm.qld.gov.au
[B] School of Natural Resources, Queensland University of Technology, Brisbane, Australia, Email r.thwaites@qut.edu.au

Abstract
This paper examines a novel approach to examining soil-landscapes for digital soil mapping by using image clustering approaches. The move to digital soil mapping is creating a paradigm shift for many soil surveyors and is relying on new tools and techniques. In Queensland, and more generally world-wide, the requirements to support many environmental objectives are "stretching" the existing land resource information base to the limits of its intended purpose when collected over the last half century. In an attempt to utilise the knowledge contained in legacy mapping of Land Systems in Queensland, image clustering techniques have been tested to identify their suitability to spatially disaggregate existing mapping. Since a Land System, is a recurring pattern of soils, terrain, geology and vegetation an approach that identifies spatial patterns and digital objects is thought to provide a method of extracting this knowledge for inclusion in digital soil mapping approaches in the Inland Burnett Catchment.

Key Words
Digital Soil Mapping, Clustering, Land Systems.

Introduction

Recent improvements in computation, information technology and the types of tools available to soil scientists have led to paradigm shift in land resource assessment. Soil survey and land resource assessment is now moving towards digital soil mapping. With digital soil mapping is moving out of the research phase to become a semi-routine technique that is used in land resource assessment (McBratney *et al*. 2003). The increased access and use of geographical information systems (GIS), digital elevation models, geophysical tools, remotely sensed data and a myriad of other datasets has created a trend towards more quantitative resource assessment. The use of new tools and techniques has raised the awareness of the need to capture and communicate the knowledge gained by surveyors (Bui 2004).

With new natural resource management requirements it has become apparent that existing qualitative and non-digital land resource information needs to be re-interpreted. The non-sustainable management of natural resources has a significant impact on our quality of life (Hillel 2000). The small-scale Land Systems mapping of Queensland and Northern Australia is a prime example of this type of data needing re-interpretation. This re-interpretation fulfils the need to provide more quantitative soil-landscape attribute information at improved scales and resolution. A digital soil-landscape process is used to disaggregate Land Systems mapping in the Burnett Catchment of South East Queensland (Figure 1).

Methods

Existing Land Resource Mapping
To overcome the lack of information available following the Second Wold War when there was increasing development pressures in Northern Australia, Christian and Stewart (1953, 1968) introduced the concept of land systems mapping. They reason that land systems mapping would allow for a reduction in effort to gather knowledge about an area but would provide a broadscale framework on which further intensive studies can be undertaken in areas where special features are important. They rationalise that a hierarchical approach to sub-dividing and describing the landscape during a reconnaissance survey is best suited to covering large tracts of land and providing a framework for the description of the landscapes. In the study area there are two existing land system mapping projects that are complemented by two 1:50,000 soil surveys.

Environmental Correlation Datasets
Several datasets for environmental correlation exist for the catchment, including a Digital Elevation Model (DEM), gamma-ray spectrometry, geology and climate data. DEMs and airborne geophysics have been shown as useful tools for predicting soil-landscape attributes in digital soil mapping (DSM) studies.

The DEM has a pixel size of 25 metres and was built in ANUDEM (Hutchinson 1989) from 1:100,000 scale topographic data that is hydrologically correct. A range of derivatives have been generated to use as environmental covariates, these include slope, topographic wetness index, relative elevation and curvatures.

While the list of DEM derivatives listed above is by no means exhaustive they have previously been found to be useful for DSM, for example Ziadat (2005) used DEM derivatives to predict soil attributes in Jordan.

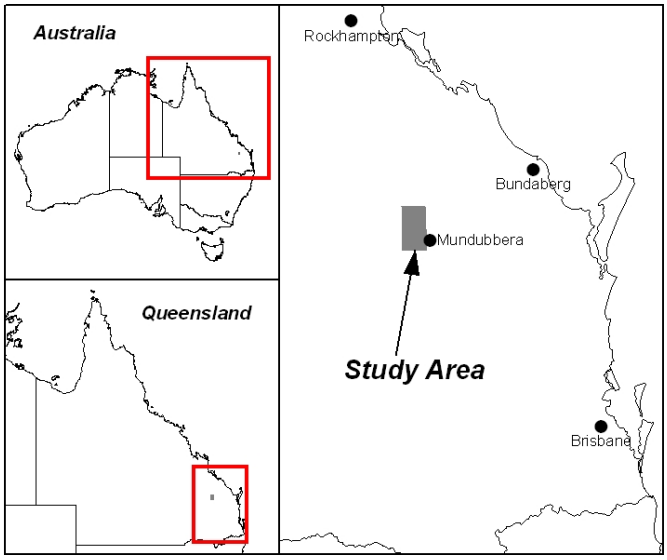

Figure 1. Study area location.

Airborne gamma-ray spectrometry (radiometrics) measures the abundance of Potassium (K), Thorium (Th) and Uranium (U) in soils by detecting the gamma-rays emitted due to the natural radioelement decay of these elements (Wilford 2002). relates to the parent material and geochemistry of the soil (and other weathered materials). Weathering modifies the distribution and concentration of radioelements compared to the original bedrock. Understanding the bedrock and soil responses has proven invaluable not only for mapping soils based on parent materials but also for understanding geomorphic processes (Wilford, Bierwirth and Craig 1997). K, Th and U behave quite differently under weathering situations. Cook *et al.* (1996) utilised radiometric data for digital soil mapping in Western Australia.

The environmental correlation datasets where analysed with both statistical methods and expert opinion as to there usefulness for clustering. The main statistical technique used was an analysis of variance and some decision tree methods to further evaluate the utility of the large number of environmental correlation layers and propose those to be used for clustering. Expert opinion was included as an overarching method to validate the statistical techniques and ensure the correlation dataset actually had a meaning to the soil surveyor.

Each of the environmental datasets required manipulation to set them to a standardised extent and cell size, but also to a standard data range (0 - 255). The standard data range ensures no one variable can significantly outweigh the others when calculating variance in "attribute space". A number of the datasets where also manipulated to adjust their distribution to limit the effects of skewed data. A prime example of this is Slope (as derived from the DEM) that has a significant skew in the towards flatter areas with a small number of high slope areas (Figure 2).

Image Clustering Method

The spatial disaggregation methodologies applied to the Inland Burnett Catchment area based on a Multiscale Object Modelling approach developed over a number of years for the analysis of remote sensing data, including medical imaging. Hay *et al.* (2005) developed a method (Multiscale Object Specific Segmentation - MOSS) which involves three specific stages in the development of a series of multiscale polygons for forest inventory. The three stages are object analysis, object upscaling and finally the merging of regions.

The merging step is named Size Constrained Region Merging (SCRM), since the regions created are determined

by a user defined size parameter and was proposed by Castilla (2003) to handle multiple bands in a Landsat Image. SCRM is an image smoothing and merging mechanism that produces features that represent individual image objects and maybe converted to a vector layer with associated attributes compiled against it.

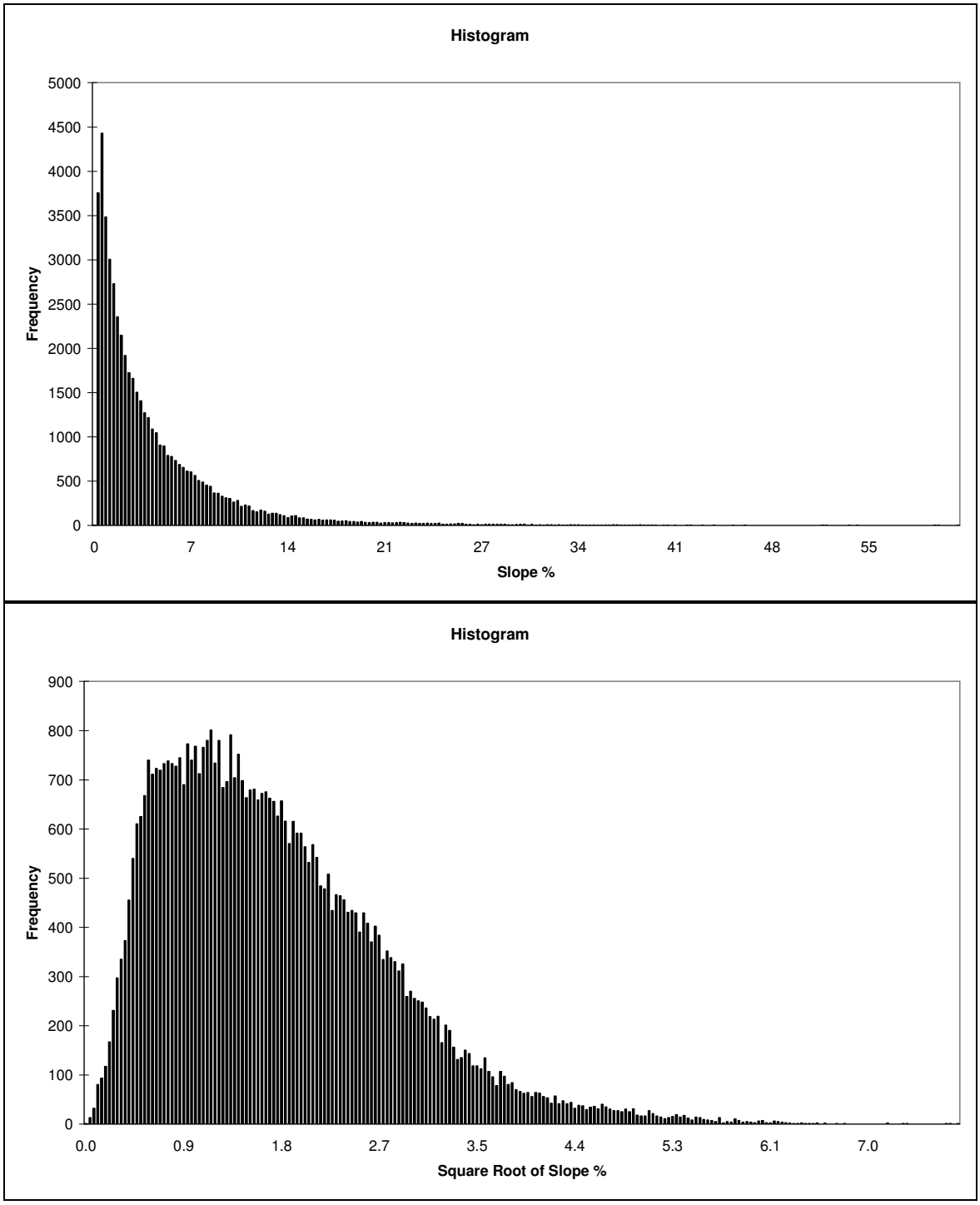

Figure 2. Histograms of DEM derived Slope percentage and the transformed slope.

Digital Soil Modelling

The most appropriate method for digital soil modelling based on image clustering techniques is still being evaluated. Several techniques exist to model and map the improved soil information in the pilot area of the Burnett Catchment. The preference for soil attribute modelling would be to use existing knowledge from land systems survey to identify areas that are known. Several methods exist for the DSM component of this project; these include the ASRIS methodology (McKenzie *et al.* 2005) to define attributes levels for soils, land units and land systems that may be complemented by extrapolation with fuzzy or Bayesian models. The use of tree based approaches used by Zhu *et al*. (2004) may also be valid, especially with the parent-child relationship that exists from the multi-scale polygons identified by the MOSS method.

Conclusion

The Multiscale Object Specific Segmentation method has the ability to provide another tool in the set of methods used for DSM. The ability to identify the environmental correlation datasets used impact greatly on the usefulness of the method. With the right layers selected, the method has the ability to rapidly dissect the landscape into units through a similar process to Air Photo Interpretation. The rapid building of landscape units has the potential to improve the speed at which DSM assessments can be undertaken in areas with existing small-scale land resource information.

References

Cook SE, Corner RJ, Groves PR, Grealish GJ (1996) Use of airborne gamma radiometric data for soil mapping. *Australian Journal of Soil Research* **34**, 183-194.

Bui EN (2004) Soil survey as a knowledge system. *Geoderma* **120**, 17-26.

Castilla G (2003) Object-oriented analysis of Remote Sensing images for land cover mapping: conceptual foundations and a segmentation method to derive a baseline partition for classification, PhD edn, Polythecnic University of Madrid, Madrid, Spain.

Christian CS, Stewart GA (1968) Methodology of Integrated Surveys. In 'Aerial Surveys and Integrated Surveys, Proceedings Toulouse Conference 1964'. Toulouse. pp. 233-280. (UNESCO).

Christian CS, Stewart GA (1953) 'General Report on Survey of Katherine - Darwin Region, 1946'. (CSIRO: Australia).

Cook SE, Corner RJ, Groves PR, Grealish GJ (1996) Use of airborne gamma radiometric data for soil mapping. *Australian Journal of Soil Research* **34**, 183-194.

Hay GJ, Castilla G, Ruiz JR, Wulder MA (2005) "An automated object-based approach for the multiscale image segmentation of forest scenes", *International Journal of Applied Earth Observation and Geoinformation* **7**(4), 339-359.

Hillel D (2000) 'Salinity Management for Sustainable Irrigation'. (World Bank Publications).

Hutchinson MF (1989) A new procedure for gridding elevation and stream line data with automatic removal of spurious pits. *Journal of Hydrology* **106**, 211-232.

McBratney AB, Minasny B, Mendonça Santos ML (2003) On digital soil mapping. *Geoderma* **117**, 3-52.

McKenzie NJ, Jacquier DW, Maschmedt DJ, Griffin EA, Brough DM (2005) *Australian Soil Resource Information System Technical Specifications, Version 1.5,* Australian Collaborative Land Evaluation Program, Canberra.

Wilford J (2002) Airborne Gamma-ray Spectrometry. In 'Geophysical and Remote Sensing Methods for Regloith Exploration'. (Ed. E Papp) pp. 46-52. (CRC LEME: Canberra, Australia).

Wilford JR, Bierwirth PN, Craig MA (1997) Application of airborne gamma-ray spectrometry in soil/regolith mapping and applied geomorphology. *AGSO Journal of Australian Geology and Geophysics* **17**, 201-216.

Zhu J, Morgan CLS, Norman JM, Yue W, Lowery B (2004) "Combined mapping of soil properties using a multi-scale tree-structured spatial model" *Geoderma* **118**(3-4), 321-334.

Ziadat FM (2005) Analyzing digital terrain attributes to predict soil attributes for a relatively large area. *Soil Science Society of America Journal* **69**, 1590-1599.

Landscape-scale sampling of forest-derived carbon in cultivated systems of East Africa

Leigh Winowiecki[A*], Markus Walsh[A], Pedro Sanchez[A]

[A] Tropical Agriculture and Rural Environment Program at the Earth Institute at Columbia University, Palisades, New York, 10964, USA, Email[*]: law2140@columbia.edu.

Abstract
Loss of natural ecosystems and the increase of annual cropping systems are inextricably linked to ecosystem function and food security. Understanding how land-use change contributes to functional soil properties such as soil organic matter cycling will help in the design of agricultural systems in order to enhance the soil ecosystem. Three Millennium Village (MV) sites (Sauri, Kenya; Ruhiira, Uganda; and Mbola, Tanzania) were chosen to develop soil organic carbon reference values at a landscape scale. Mbola site was further selected to construct a chronosequence to calculate organic matter turnover rates on two different soil types prevalent across the landscape. These three sites represent distinct forest types and are at various stages along the restoration-degradation pathway. The Land Degradation Surveillance Framework (LDSF) developed by Markus Walsh and Tor Vagen was used to sample the landscape and is a stratified random sampling design that uses a nested spatial hierarchy. Soil organic carbon (SOC) and stable carbon isotopes were measured on 171 composite soil samples from 0-20 cm and 20-50 cm depths. Paired sampling of forested and cultivated sites at the Mbola village was conducted and soil pits were excavated to classify and describe soil. Multilevel models were used to analyse variance within the hierarchy and to model parameters at different spatial scales. SOC, sand content, carbon isotope signatures varied between the three sites. SOC reference values and SOM turnover rates will be calculated and presented.

Key Words
Stable carbon isotopes, SOC, SOM.

Introduction
Loss of natural ecosystems, diminishing ecosystem function, and the prevalence of non-replenishing cropping systems are inextricably linked to food security. It is estimated that while 70% of Africa's population live in rural areas and depend almost solely on agriculture, over half of Africa's land is unsuitable for agriculture (Swift and Shepherd 2007). Degradation of soil and water resources is suggested to inhibit the needed increase in food production in sub-Saharan Africa (Verchot *et al.* 2005). Understanding how land-use change contributes to functional soil properties such as soil organic matter cycling may help in the design of agricultural systems in order to enhance the soil ecosystem. Soil provides multiple ecosystem services (i.e. medium for plant and agricultural production, filtering of toxins and pollutants and regulating the hydrologic cycle) (Millennium Ecosystem Assessment 2005). Specifically, soil organic matter (SOM) is described as one for the three core soil properties contributing to soil function (Palm *et al.* 2007). Its depletion or degradation can have serious impacts on aboveground productivity. Yet, the impacts of land-use change on SOM cycling in sub-Saharan Africa are still understudied. A landscape-scale understanding of SOM dynamics, beyond carbon stock calculations, is lacking, particularly in areas where smallholder farmers critically need this information most. Creating regional SOC reference values for semi-natural and cultivated sites across a landscape will help guide management recommendations and provide useful information about basic ecosystem function for a converted landscape. In addition, calculating soil organic matter turnover rates will improve our understanding of effects of forest conversion on the carbon cycle.

Soil Organic Matter Dynamics
Stable carbon isotope signatures in the soil allude to vegetation composition because photosynthetic pathways of plants discriminate against the heavier carbon isotope differently. Most plants and trees, use the C3 (Calvin cycle) photosynthetic pathway and have a more negative $\delta^{13}C$ value compared to maize and other cereal crops and grasses which utilize the C4 (Hatch-Slack) pathway. Stable carbon isotopes have been used to determine the SOM turnover rates at local scales (Balesdent and Mariotti 1996, Bernoux *et al.* 1998), identify vegetative sources of organic matter to the soil (Roscoe *et al.* 2001, Krull *et al.* 2007), and address the impact of land conversion on soil condition (Vagen *et al.* 2006, Awiti *et al.* 2008, Schulp and Veldkamp 2008). This project will build on these studies by comparing three different forest types and utilizing a spatially balanced sampling

design to understand landscape-scale SOM dynamics.

Methods

Three Millennium Village (MV) sites (Sauri, Kenya; Ruhiira, Uganda; and Mbola, Tanzania) were sampled because they represent three distinct forest types and have varying degrees of land-use change (Table One). The Land Degradation Surveillance Framework (LDSF) developed by Markus Walsh and Tor Vagen was used to collect soil samples across the study sites. LDSF is a stratified random sampling design using a nested spatial hierarchy (Figure 1). Composite soil samples were taken from four subplots within each plot from 0-20-cm and 20-50-cm depths. Soil samples were air dried and sieved to 2 mm. One hundred and seventy-one soil samples were analysed for stable carbon isotopes and soil organic carbon with a stable-isotope-ratio mass spectrometer on whole soil samples at Iso-analytical Laboratories in the UK (http://www.iso-analytical.co.uk/). Isotope results are reported in standard delta notation relative to a Pee-Dee Belemnite (PDB) standard. Twenty percent of the samples received a duplicate analysis for quality control.

Table One. Millennium Village Site Descriptions.

MV Site	Forest Type	Where on the degradation/restoration pathway
Mbola, Tanzania	Miombo Woodland	Land conversion still occurring
Ruhiira, Uganda	Sub-humid highland forest	Deforested
Sauri, Kenya	Humid/sub-humid forest	Was deforested, tree plantings are occurring

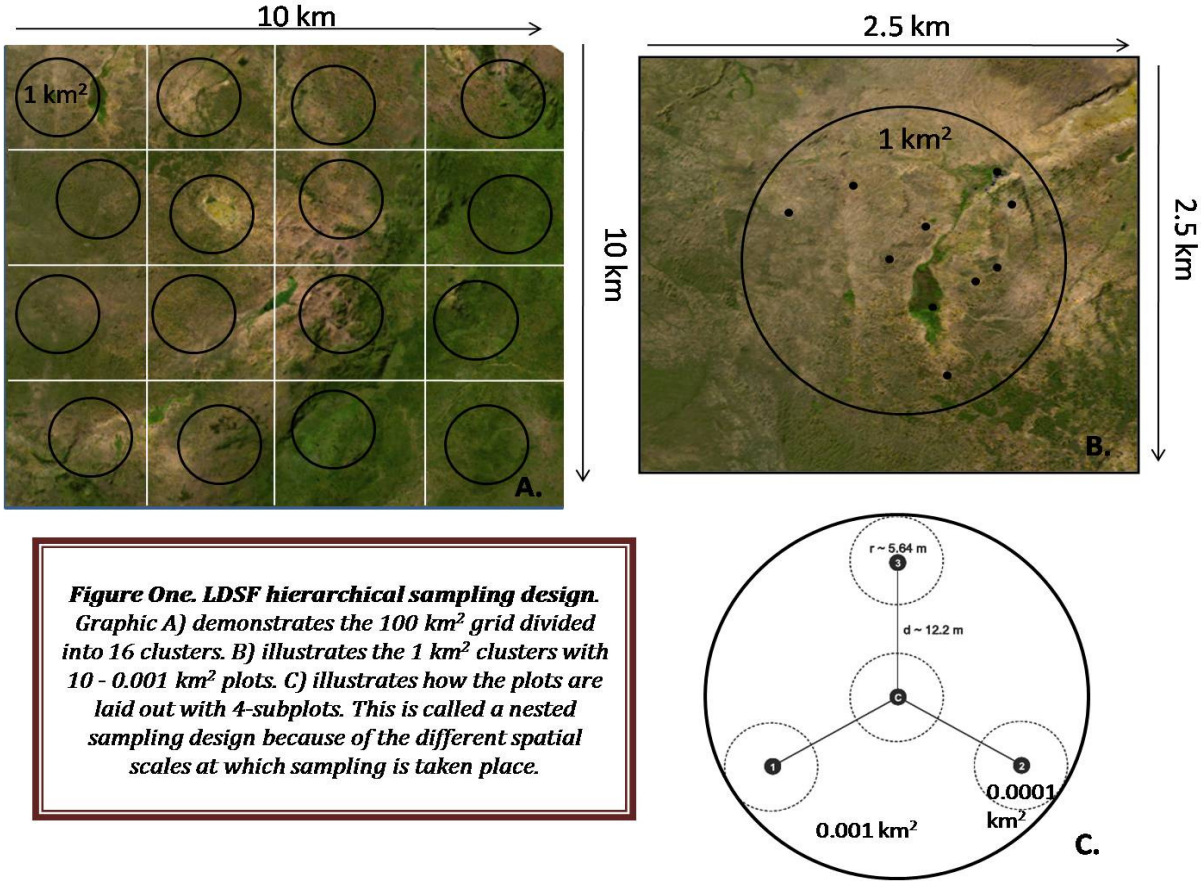

Figure One. LDSF hierarchical sampling design. Graphic A) demonstrates the 100 km² grid divided into 16 clusters. B) illustrates the 1 km² clusters with 10 - 0.001 km² plots. C) illustrates how the plots are laid out with 4-subplots. This is called a nested sampling design because of the different spatial scales at which sampling is taken place.

Figure 1. Land Degradation Surveillance Framework sampling design.

Chronosequence Soil sampling

To compliment this sampling strategy, eight new paired sites, forest and cultivated sites with known time since conversion, were selected and sampled within LDSF framework at the Mbola, Tanzania Millennium Village to calculate SOM turnover rates for the Miombo Woodland region. Farmer interviews provided information on land-use history including time since conversion for the cultivated sites. Soil pits were excavated and soils at

each paired site were classified using Soil Taxonomy and World Reference Base to ensure morphological homogeneity within the paired sites. Undisturbed soil cores were taken to determine bulk density at three depths 0-20, 20-50, and 50-100 cm.

Calculations and Statistical Modelling

Soil organic carbon reference values will be calculated controlling for sand content for each of the sites and presented for the landscape. Soil organic matter turnover rates will be calculated along a chronosequence of land use using stable carbon isotope values and time since conversion using linear mixed effect models performed in the statistical package R. These data will allow us to compute the percent of tree-derived carbon in the soil along a chronosequence of time since conversion.

Preliminary Results

Total soil organic carbon contents and sand content were clustered for the three villages (Figure 2). Mbola, TZ site had the highest sand content and lowest SOC values. Delta carbon 13 values for top and sub soil at each of the village sites indicate the prevalence of mixed C3-C4 systems.

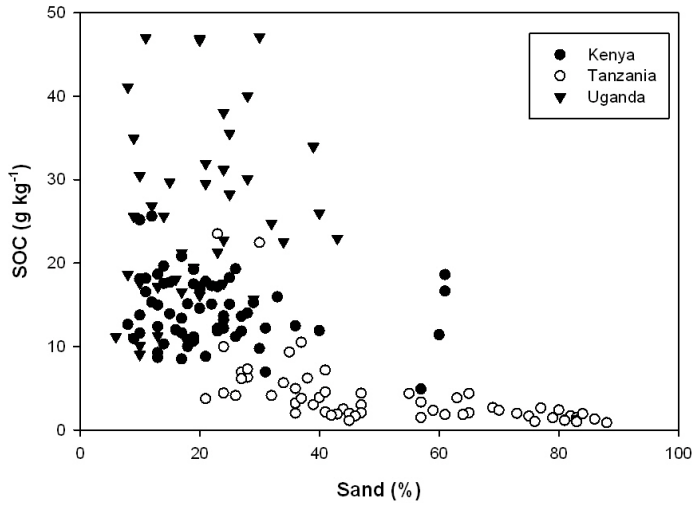

Figure 2. SOC vs sand for top and subsoil samples at the three Millennium Village Sites.

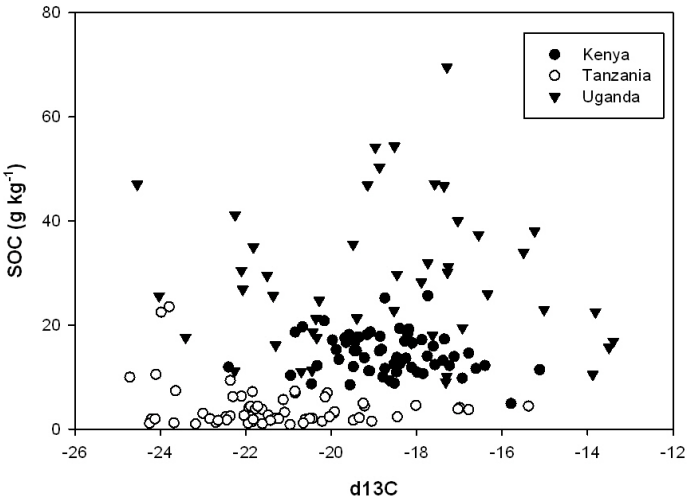

Figure 3. SOC vs $\delta^{13}C$ values for top and subsoil samples at the three Millennium Village Sites.

References

Awiti A, Walsh M, Shepherd K, Kinyamario J (2008) Soil condition classification using infrared spectroscopy: A proposition for assessment of soil condition along a tropical forest-cropland chronosequence. *Geoderma* **143,** 73-84.

Balesdent J, Mariotti A (1996) Measurement of soil organic matter turnover using C-13 natural abundance. Pages 83-111 *in* T. W. Boutton and S. Yamasaki, editors. Mass Spectrometry of Soils. Marcel-Dekker, New York.

Bernoux M, Cerri C, Neill C, de Moraes JFL (1998) The use of stable carbon isotopes for estimating soil organic matter turnover rates. *Geoderma* **82,** 43-58.

Krull E, Bray S, Harms B, Baxter N, Bol R, Farquhar G (2007) Development of a stable isotope index to assess decadal-scale vegetation change and application to woodlands of the Burdekin catchment, Australia. *Global Change Biology* **13,** 1455-1468.

Millennium Ecosystem Assessment (2005) Ecosystem and Human Well-being Synthesis. Island Press, Washington DC.

Palm C, Sanchez P, Ahamed S, Awiti A (2007) Soils: A contemporary perspective. *Annual Review of Environmental Resources* **32,** 99-129.

Roscoe R, Buurman P, Velhorst EJ, and V. C.A (2001) Soil organic matter dynamics in density and particle size fractions as revealed by the $^{13}C/^{12}C$ isotopic ratio in Cerrado's Oxisol. *Geoderma* **104,**185-202.

Schulp CJE, Veldkamp A (2008) Long-term landscape – land use interactions as explaining factor for soil organic matter variability in Dutch agricultural landscapes. *Geoderma* **146,** 457-465.

Swift MJ, Shepherd K (2007) Saving Africa's soil: Science and technology for improved soil management in Africa. World Agroforestry Centre, Nairobi.

UNEP (in press) Land Health Surveillance: An Evidence-Based Approach to Land Ecosystem Management. Illustrated with a Case Study in the West Africa Sahel. Nairobi.

Vagen T, Walsh M, and Shepherd K (2006) Stable isotopes for characterisation of trends in soil carbon following deforestation and land use change in the highlands of Madagascar. *Geoderma* **135,**133-139.

Verchot L, Mackensen J, Kandji S,Van Noordwijk M, Tomich T, Ong C, Albrecht A, Bantilan C, Anupama KV, Palm C (2005) Opportunities for linking adaptation and mitigation in agroforestry systems *in* Robledo C, Kanninen M, Pedroni L, editors. Tropical forests and adaptation to climate change: In search of synergies. Center for International Forestry Research (CIFOR), Bogor.

Modelling N mineralization from green manure and farmyard manure from a laboratory incubation study

M. Mohanty[A,C,E], M. E. Probert[B], K. Sammi Reddy[C], R.C. Dalal[A,D4], A. Subba Rao[C] and N. W. Menzies[A]

[A]School of Land, Crops and Food Sciences, The University of Queensland, Australia 4072.
[B]CSIRO Sustainable Ecosystems, Queensland Bioscience Precinct, 306 Carmody Road, Australia 4067.
[C]Indian Institute of Soil Science, Nabibagh, Berasia Road, Bhopal, India 462038.
[D]Queensland Department of Environment and Resource Management.
[E]Corresponding author. Email m.mohanty@uqconnect.edu.au

Abstract
Predicting N mineralization from farmyard manure (FYM) is more difficult than from crop residues as manures vary greatly in composition. A laboratory incubation experiment was carried out for 98 days at 30º C under aerobic conditions to study the effects of gliricidia (*Gliricidia sepium*), a green manure crop and FYM applied to soil at 5 and 10 g/kg. Application of gliricidia induced N mineralization from the start of incubation process being greater at higher rate of application. Application of FYM increased immobilization of mineral N in soil irrespective of the rates of application; the mineral N in soil was completely immobilized within 2 weeks for the 10 g/kg rate. The initial net immobilization from FYM was limited by availability of N in the soil for the higher rate of application. We used the APSIM SoilN module to simulate N mineralization from these manures. The prediction of N mineralized from gliricidia was better than FYM. Results from the study indicated that existing SOILN module with the pools (FPOOLs) having the same C:N ratio did not work well in predicting the N mineralization from FYM. Poor prediction of N mineralized from FYM could be overcome by modifying the individual pools (FPOOL1, FPOOL2 and FPOOL3) and the pools C:N ratios. The modelling efficiency, a measure of goodness of fit between the simulated and observed data, improved significantly for the modified model.

Key Words
Farmyard manure, nitrogen, mineralization/immobilization, modelling, APSIM.

Introduction

The N mineralization from crop residues is influenced by the concentration of N, hemicelluose, lignin and ratios of chemical components such as C:N. Manures are different from crop residues as they vary greatly in composition (Lekasi *et al.* 2003), being a complex mixture of animal excreta and plant residues, with varied mineralization kinetics ranging from relatively resistant lignin to readily available NH_4^+ and volatile fatty acids (Van Kessel *et al.* 2000). Van Kessel *et al* (2000) reported that manure contains a range of compounds that have rapid or intermediate N mineralization characteristics, or that are strong immobilizers of N and suggested that improved estimates of manure N mineralization may be obtained by considering both the readily available N components and components that strongly immobilize N.

Models differ in the pool structure used to describe the decomposition of organic inputs, with the pools differing in their rates of decomposition. The assumption that all pools have the same C:N ratio may fail to adequately represent the observed behaviour of organic manures. Probert *et al.* (2005) found that predicting N mineralization from such a complex mixture was difficult with the existing models, and reported N mineralization from different feed and faecal materials from Africa as predicted by Agricultural Production Systems Simulation Model (APSIM). The APSIM SoilN module was modified based on varying C and N in different pools that make up the added organic matter. It was shown that the revised model was better able to simulate the general patterns of N mineralized that has been reported for various organic sources. To be able to predict N release from manures more efficiently, it is necessary that the model is flexible enough to simulate the N mineralization from different types of organic manures available in different parts of the world. In this study we used two sources of organic manures viz., green manures (*Gliricidia sepium,* material with low C:N ratio and easily decomposable in soil) vs. the farmyard manure (FYM) from subtropical India which is a more complex mixture than green manure in terms of quality and N mineralization pattern. This study was intended to provide an insight to N mineralization modeling from organic manures which are different in their biochemical properties (as well as C:N ratio) from the materials studied by Probert *et al.* (2005). In this study, the SoilN module of APSIM (v 5.2) has been used.

1 – 6 August 2010, Brisbane, Australia. Published on DVD.

Materials and methods

Green manures and farmyard manure

The study was conducted using the field-moist soil from the top (0-15 cm) layer of a cultivated Vertisol (Bhopal, India at 23° 18' N and 77° 24' E). The incubation studied N mineralization from green manure (gliricidia) and FYM, using two rates of application, 5 g/kg and 10 g/kg. The properties of the gliricidia and FYM are given in Table 1.

Table 1. Biochemical composition of the organic manures used for simulation study.

Treatment	Overall C/N ratio	Proportion of C in FPOOLs (%)			C:N ratio of FPOOLs		
		Pool 1	Pool 2	Pool 3	Pool 1	Pool 2	Pool 3
FYM (UM)	30	20	70	10	30	30	30
FYM (M	30	9	73	18	50	44	12

* UM: unmodified; M: modified

Analytical procedures

The soil used in the incubation study had pH 8.1(in 1:2.5 soil:water suspension), organic C content of 5.1 g/kg, a C:N ratio 9.6, and inorganic N (NH_4-N and NO_3-N) content of 30 mg/kg. Total N was determined using the semi-micro Kjeldahl method of Bremner and Mulvaney (1982). Total C in organic materials was estimated by the weight loss on ignition. Lignin in the organic materials was determined using the acid detergent fibre (ADF) method as outlined by Rowland and Roberts (1994). Total soluble polyphenols in organic materials was determined by the Folin-Ciocalteau method (Constantinides and Fownes 1994).

Laboratory Incubation experiment

Finely ground gliricidia twigs (leaves and succulent stem) and FYM (collected from a typical Indian farm) were applied to soil at two rates of application, 5 g/kg and 10 g/kg on an oven dry-weight basis.

For each treatment, a sample of 500 g soil was hand mixed with 2.5 g or 5.0 g of organic material (depending upon the rate of application), then transferred to a plastic bottle. The control treatment was soil without added organic materials. The treatment mixtures were maintained at field capacity throughout the incubation period by replacing any loss of water with the appropriate volume of distilled water at every sampling. The soil and organic material mixtures were incubated at 30±2 °C for 14 weeks in duplicate in a laboratory incubator. Soil samples were taken at 0, 1, 2, 4, 6, 8, 10, 12 and 14 weeks and analyzed immediately for inorganic N (NH_4-N + NO_3-N) using 2M KCl extraction followed by distillation. Net N mineralized during the incubation process was calculated as follows:

$(\text{Net N mineralized from organic materials})_t = (\text{Mineral N in the treatment} - \text{mineral N in control})_t$.

Modelling decomposition of organic materials and release of nitrogen

Description of the APSIM SoilN module

The APSIM SoilN module (APSIM v 5.2) represents the decomposition of organic inputs as influenced by the quality of organic inputs. The effect of changing the pool structure and C:N ratio of individual pools on decomposition of organic materials has been described by Probert *et al.* (2005). The APSIM SoilN module was modified so that the three pools that constitute added organic matter could be specified in terms of both the fraction of C in each pool and also their C:N ratios. The model was parameterized by associating the model parameters with measured properties (the pool that decomposes most rapidly equates with water-soluble C and N; the pool that decomposes slowest equates with lignin-C). Then the model was evaluated for N mineralized from gliricidia and FYM from a laboratory incubation study.

Model evaluation

The performance of APSIM simulation for prediction of net N mineralized from the application of these high C:N ratio materials was evaluated using two statistics: (i) the root mean square error (RMSE), and (ii) the modelling efficiency (EF) (Smith *et al.* 1996).

Results and discussion

Nitrogen mineralization from gliricidia and farmyard manure

Total C content of the gliricidia was 40, while total N was 3.72% and hence, the C:N ratio of 11. The lignin content of the materials was 6.5% and that of polyphenols was 1.5%. The C:N ratio of FYM used for the study was 30 with lignin and polyphenols content being 11 and 1.22%. The C:N ratio of the water soluble component of FYM was 50. The application of gliricidia caused net N mineralization in soil which increased with time and

with the rates of application (Figure 1). With increase in incubation period the difference in N mineralized between two rates of application became bigger. At the end of the incubation period, about 65% of applied N was mineralized for the 5 g/kg rate while the N mineralized from the 10 g/kg rate was 54%.

With increase in incubation period, the amount of N immobilized from FYM was greater from the higher rate of application, and N immobilization continued till the end of the incubation period (Figure 1). The amount of N immobilized from the application of low rate (5 g/kg) of FYM was limited by C availability where as at higher rate (10 g/kg), it was limited by mineral N. Increasing the rates of application of FYM caused more immobilization of available N in soil system indicating utilization of available N by microbes from the soil environment when decomposing organic materials with high C:N ratio (Alexander 1977).

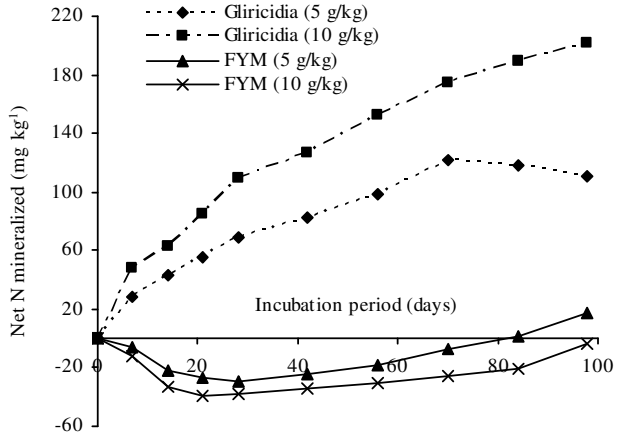

Figure 1. Net N mineralization from gliricidia and FYM under different rates of application.

Modelling N mineralized from gliricidia and farmyard manure

The comparison of simulations with measured data for different rates of application gliricidia is shown in Figure 2 (a,b). The pattern of N mineralized as seen in the observed data was well presented by the model. The amount of N mineralized as predicted by the model from the 10 g/kg rate of gliricidia was twice the amount N mineralized from the application of 5 g/kg. The model will predict that N mineralization from gliricidia depends on its C:N ratio, so that net N mineralized is directly proportional to rate of application. But this trend was not obtained from the observed data. Based on the pattern of N mineralization and the statistics used for the evaluation of the model the goodness of fit was quite satisfactory for gliricidia (EF = 0.87).

The simulation of N mineralized from different rates of application of FYM was presented in Figure 3a and 3b. Assuming that added C in the three FPOOLs of the model is always in the proportion of 0.2-0.7-0.1 (as defined in the model for crop residues and roots), the simulation of N immobilized from both the rates of

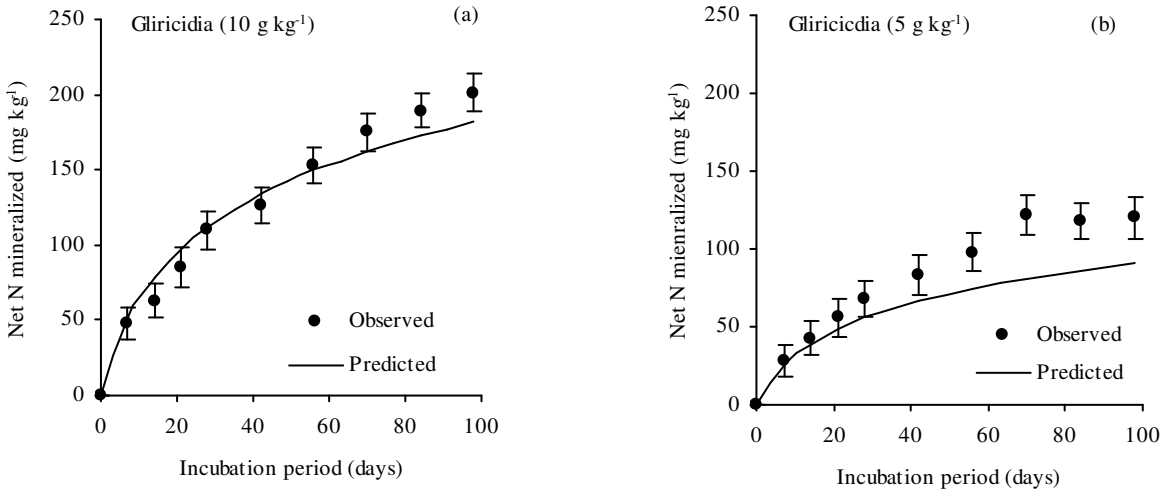

Figure 2. Net N mineralization from gliricidia under different rates of application as predicted by the model.

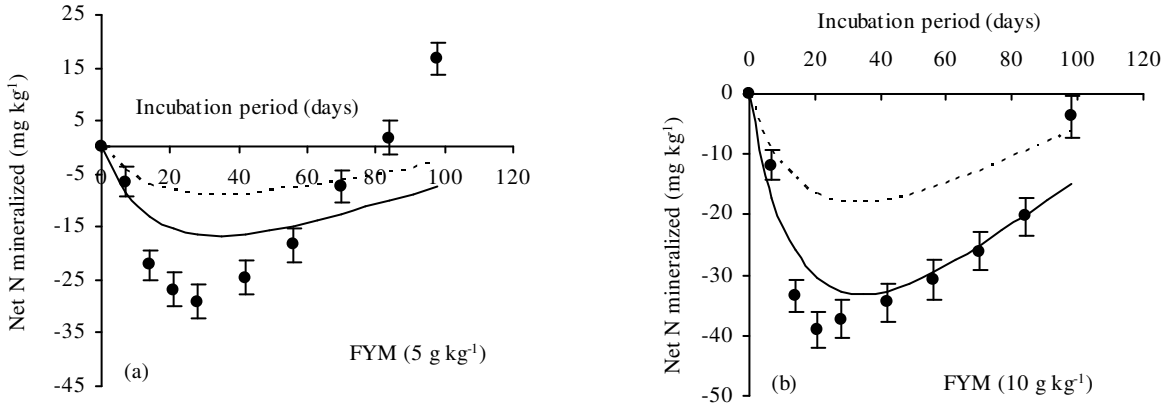

Figure 3. Net N mineralization from FYM at two rates of application. Experimental data shown as symbols with bar representing ± standard errors. The dotted line is for the un-modified model, where all organic material is assumed to decompose with the same C:N ratio; the continuous line is for the modified model with different C:N ratio in each FPOOL. The parameters used to specify the proportion of C and C:N in the three FPOOLs are given in Table 1.

FYM as predicted by the model (un-modified version) was shown in Figure 3. The goodness of fit was very poor for both the rates of application (RMSE = 14.69, EF = 0.05). When "FPOOLs" were specified in similar manner to that suggested by Probert *et al.* (1995) (see Table 1), the goodness of fit was better than the unmodified model (RMSE = 9.24, EF = 0.62).

The model assumes the water soluble component of C and N as FPOOL1 and thus, from the analytical results, it was possible to determine the proportion of C in this pool and its C:N ratio (Table 1). This enabled us to achieve an acceptable fit to the observed data. We also assume that acid detergent lignin, which is proximate analysis of lignin, equates to FPOOL3, permitting the fraction of C in this pool to be estimated. The fraction of C in FPOOL2 was found by difference. Since, the overall C:N ratio (on a total dry matter basis) is also known, the only missing information was the distribution of water insoluble N between FPOOL2 and 3. A series of simulations were carried out for the FYM with different combinations of C:N in the two pools. To obtain a goodness of fit shown in Figure 3, the manure required C:N ratio of FPOOL1 to be set to 50, FPOOL2 to 44, with the corresponding C:N ratio in FPOOL3 of 12. For FYM, the goodness of fit is substantially better in the modified model than the unmodified one.

References

Alexander M (1977) 'Introduction to Soil Microbiology' .2nd edition. (John Wiley and Sons: New York).

Bremner JM, Mulvaney CS (1982) Nitrogen - Total. In 'Methods of Soil Analysis'. (Eds AL Page, RH Miller, DR Keeney) pp. 595-617. (ASA-SSSA, Madison, WI).

Constantinides M, Fownes JH, (1994) Nitrogen mineralization from leaves and litter of tropical plants; relationship to nitrogen, lignin and soluble polyphenol concentrations. *Soil Biol Biochem* **26,** 49–55.

Korsaeth A, Molstand L, Bakka LR (2001) Modelling the competition for nitrogen between plants and micro-flora as a function of soil heterogeinity. *Soil Biol Biochem* **33,** 215-226.

Lekasi JK, Tanner JC, Kimani SK, Harris PJC, (2003) Cattle manure quality in Maragua district Central Kenya: effect of management practices and development of simple methods of assessment. *Agriculture Ecosystem Environment* **94,** 289-298.

Probert ME, Delve RJ, Kimani SK, Dimes JP (2005) Modelling nitrogen mineralization from manures: representing quality aspects by varying C:N ratio of subpools. *Soil Biol Biochem* **37,** 279-287.

Recous S, Robin D, Darwis D, Mary B (1995) Soil inorganic N availability: effect on maize residue decomposition. *Soil Biol Biochem* **12,** 1529-1538.

Smith J, Smith P, Addiscott T (1996) Quantitative methods to evaluate and compare soil organic matter models. In 'Evaluation of soil organic matter models'. (Eds DS Powlson *et al.*) pp. 181–199. (Springer-Verlag: Berlin).

Van Kessel JS, Reeves JB, Meisinger JJ (2000) Nitrogen and carbon mineralization of potential manure components. *Journal of Environtal Quality* **29,** 1669–1677.

Modelling N mineralization from high C:N rice and wheat crop residues

M. Mohanty[A,C,E], M. E. Probert[B], K. Sammi Reddy[C], R.C. Dalal[A,D4], A. Subba Rao[C] and N. W. Menzies[A]

[A]School of Land, Crops and Food Sciences, The University of Queensland, Australia 4072.
[B]CSIRO Sustainable Ecosystems, Queensland Bioscience Precinct, 306 Carmody Road, Australia 4067.
[C]Indian Institute of Soil Science, Nabibagh, Berasia Road, Bhopal, India 462038.
[D]Queensland Department of Environment and Resource Management.
[E]Corresponding author. Email m.mohanty@uqconnect.edu.au

Abstract
The processes of N mineralization and immobilization which occur in agricultural soils during decomposition of crop residues are important for N dynamics in cropping systems. A laboratory incubation experiment was carried out for 98 days at 30º C under aerobic conditions to study the effects of rice (*Oryza sativa*, L.) and wheat (*Triticum aestivum*, L.) straw applied at 5 and 10 g/kg in the presence or absence of additional N (as urea). The study showed an interactive effect between the rate of application of the residues and additional N. We used the APSIM SoilN module to simulate the mineralization of N from crop residues and compared the predictions with the observed data from our incubation study. Model performance was satisfactory, and the model was able to simulate the observed interaction between rate of application of residue and added N.

Key Words
Nitrogen, mineralization/immobilization, rice straw, wheat straw, simulation modelling, APSIM.

Introduction
In the absence of recent additions of fresh organic matter, soils generally exhibit mineralization during incubations. When residues are added, the net mineralization due to the added materials can be estimated as the difference between the amended soil and a control (without amendment). Residues with low C:N ratio tend to exhibit net N mineralization, while residues with high C:N ratio exhibit immobilization (Van Kessel *et al.* 2000; Qian and Schoenau 2002). In farming systems where the straw remains on the field after harvest, its rapid decomposition is important to minimize negative effects on the following crops caused by N immobilization (Cheshire *et al.* 1999; Henriksen and Breland 1999). Yield depression following straw incorporation has been mitigated by adding inorganic N (Azam et *al.* 1991). Strategies for management of high C:N ratio residues could be improved though the use of simulation models. The objective was to evaluate the performance of APSIM to simulate the N mineralization pattern from high C:N ratio crop residues (rice and wheat straw) using a dataset from a laboratory incubation experiment that investigated the effects of rate of addition of residues with high C:N ratio, and added N, on the net N mineralization.

Materials and methods
Soil and crop residues
The study was conducted using the field-moist soil from the top (0-15 cm) layer of a cultivated Vertisol (Bhopal, India at 23° 18' N and 77° 24' E). The incubation studied N immobilization from two crop residues, rice and wheat straw, using two rates of application and in the presence and absence of added N. The C:N ratio of rice was 86 and that of wheat was 79.

Analytical procedures
A portion of field-moist soil was taken for laboratory incubation, while another portion was air-dried, crushed to pass through a 2 mm sieve, then stored in an air-tight plastic container at room temperature. A sub-sample of this material was finely ground to pass 100-mesh sieve. The soil used in the incubation study had pH 8.1 (in 1:2.5 soil:water suspension), organic C content of 5.1 g/kg, a C:N ratio 9.6, and inorganic N (NH_4-N and NO_3-N) content of 30 mg/kg. Total N using the semi-micro Kjeldahl method of Bremner and Mulvaney (1982). Total C in organic materials was estimated by the weight loss on ignition (Nelson and Sommer 1982).

Laboratory Incubation experiment
Finely ground wheat and rice straw were applied to soil at two rates of application, 5 g/kg and 10 g/kg on an oven dry-weight basis. The amount of urea-N added was enough to raise the wheat straw N to approximately 2% on dry weight basis. This required the addition of 66 mg N/kg soil where the materials were added at low rate of addition i.e. 5g/kg, and 132 mg/kg at the high rate.

For each treatment, a sample of 500 g soil was hand mixed with 2.5 g or 5.0 g of organic material (depending upon the rate of application), then transferred to a plastic bottle. For each treatment urea-N was added as appropriate. The control treatment was soil without added organic materials. The treatment mixtures were maintained at field capacity throughout the incubation period by replacing any loss of water with the appropriate volume of distilled water at every sampling. The soil and organic material mixtures were incubated at 30°C for 14 weeks in duplicate in a laboratory incubator. Soil samples were taken at 0, 1, 2, 4, 6, 8, 10, 12 and 14 weeks and analyzed immediately for inorganic N (NH_4-N + NO_3-N) using 2M KCl extraction followed by distillation (Bremner 1965). Net N mineralized during the incubation process was calculated as follows:

(Net N mineralized from organic materials)$_t$ = (Mineral N in the treatment – mineral N in control)$_t$ - N added.

Model evaluation
The performance of APSIM simulation for prediction of net N mineralized from the application of these high C:N ratio materials was evaluated using two statistics: (i) the root mean square error (RMSE), and (ii) the modelling efficiency (EF) (Smith *et al.* 1996).

Results and discussion
N mineralization from rice and wheat straw under laboratory incubation
Similar results were obtained for N mineralization from both rice and wheat straw for both the rates of application and where urea-N was added (in Figure 1 only the data for the rice treatments are shown). Application of rice straw at 5 g/kg reduced the mineral N in the soil to zero (Figure 1). Increasing the rate of rice straw application increased the time that the mineral N in soil was maintained at very low concentration. When urea-N (66 mg N/kg) was added along with 5 g/kg of straw, the mineral N in soil was not reduced to zero.

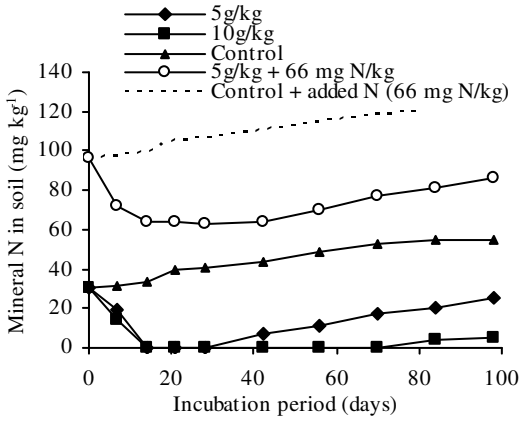

Figure 1. Nitrogen mineralization from rice straw under different rates of application. The doted line for control with 66 mg N/kg assumes all added N remain in the system.

In the absence of added N, application of 5 g/kg rice straw caused rapid immobilization which reached about 40 mg N/kg by 28 days (Figure 2a). At this time there was no mineral N in these systems (Figure 1). The disappearance of mineral N in the soil system was caused by microbial immobilization as reported by Recous *et al.* (1995). Increasing rates of straw addition increased both the amount of N immobilized and the length of the period of net immobilization (Figure 2b).

For the 5 g/kg rate of application of rice straw, adding additional N caused a small increase in the maximum amount of N immobilized (Figures 2a, c). There was no mineral N in the system at two weeks when straw was applied alone, whereas when N was added, mineral N was present throughout the incubation (Figure 1). The results obtained in our study also showed that additions of N had significant effects on net amounts of N immobilized as a result of added straw (Figure 2d). Similar results were obtained for wheat.

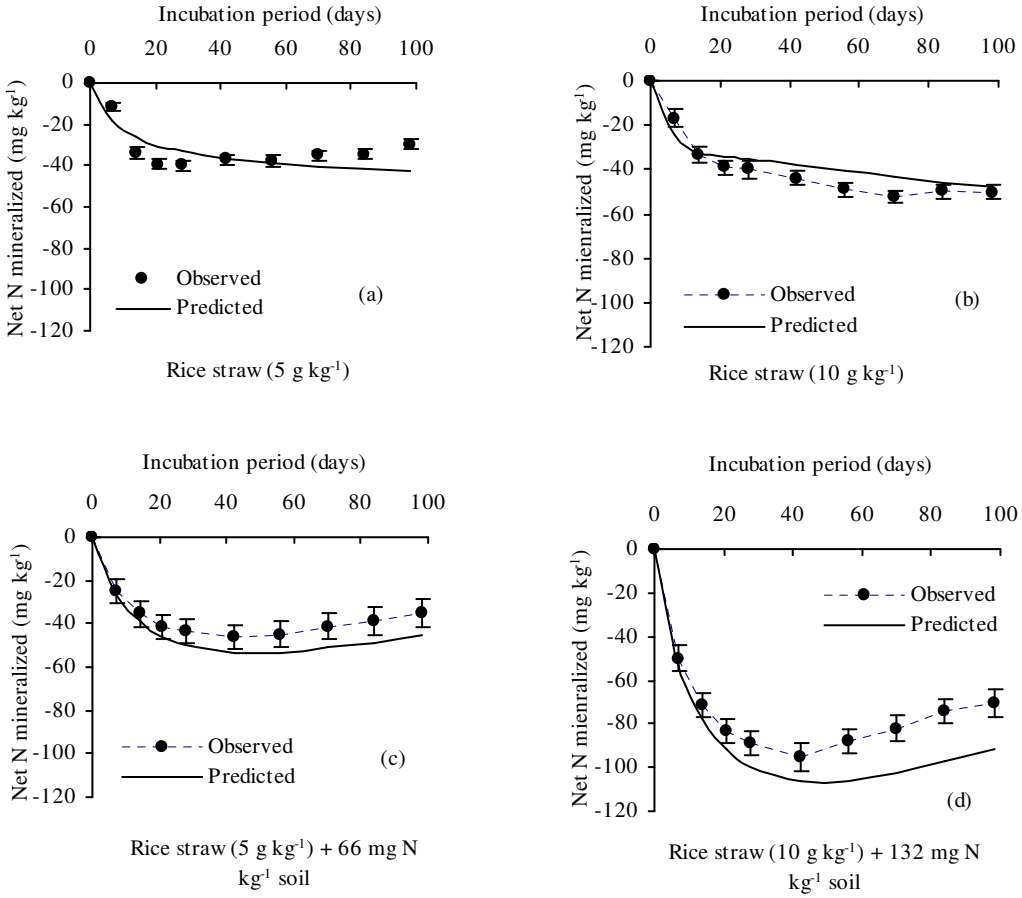

Figure 2. Simulation of net N mineralized from rice straw at (a and b) different rates of application, and (c and d) in presence of urea-N. Vertical bars represent ±standard errors.

Simulation of N mineralized from rice and wheat straw

We used the model to simulate the effect of rates of organic matter and N application, on N mineralization from high C:N ratio materials (rice and wheat straw). The APSIM model predicted N mineralization from high C:N rice straw satisfactorily under different rates of application of straw in presence and absence of added N (Figure 2). Similar observations were also recorded from wheat straw. However, in presence of added N, the model prediction was better than for the treatments with residue alone (RMSE = 10.23 and EF = 0.79) values. The model assumes that the rate of decomposition of added organic materials is limited when there is inadequate mineral N in the system to satisfy the immobilization demand. Even so, it is shown that the model predicted satisfactorily the observed behaviour of the system. The modelling efficiency, a measure of goodness of fit between the simulation and observed data, was 0.82 for the treatments in the incubation study.

Conclusion

From the incubation experiment, the high C:N ratio rice and wheat straw caused immobilization of soil mineral N, to the extent dependent on the rate of application of the straw, and the soil inorganic N availability and the APSIM model predicted it satisfactorily.

References

Alexander M (1977) 'Introduction to Soil Microbiology' .2nd edition. (John Wiley and Sons: New York).

Azam F, Lodhi A, Ashraf M (1991) Availability of soil and fertilizer N to wetland rice following wheat straw amendment. *Biology and Fertility of Soils* **11,** 97-100.

Bremner JM (1965) Inorganic forms of nitrogen. *Agronomie* **9,** 1179-237.

Bremner JM, Mulvaney CS (1982) Nitrogen - Total. In 'Methods of Soil Analysis'. (Eds AL Page, RH Miller, DR Keeney) pp. 595-617. (ASA-SSSA, Madison, WI).

Chesire MV, Bedrock CN, Williams BL, Chapman SJ, Solntseva I, Thomsen I (1999) The immobilization of nitrogen by straw decomposition in soil. *European Journal of Soil Science* **50,** 329,-341.

Van Kessel JS, Reeves JB, Meisinger JJ (2000) Nitrogen and carbon mineralization of potential manure components. *Journal of Environmental Quality* **29,** 1669-1677.

Henriksen TM, Breland TA (1999) Evaluation of criteria for describing crop residues degradability in a model of carbon and nitrogen turnover in soil. *Soil Biology and Biochemistry* **31,** 1135-1149.
Nelson DN, Sommer LE (1982) Total carbon, organic carbon and organic matter. In 'Methods of soil analysis. Part 2'. (Eds AL Page, RH Miller, DR Keeney) pp. 539-579. (American Society of Agronomy Inc.: Madison, WI)
Probert ME, Delve RJ, Kimani SK, Dimes JP (2005) Modelling nitrogen mineralization from manures: representing quality aspects by varying C:N ratio of subpools. *Soil Biology and Biochemistry* **37,** 279-287.
Qian P, Schoenau J (2002) Availability of nitrogen in solid manure amendments with different C:N ratios. *Canadian Journal of Soil Science* **82,** 219–225.
Recous S, Robin D, Darwis D, Mary B (1995) Soil inorganic N availability: effect on maize residue decomposition. *Soil Biology and Biochemistry* **12,** 1529-1538.
Smith J, Smith P, Addiscott T (1996) Quantitative methods to evaluate and compare soil organic matter models. In 'Evaluation of soil organic matter models'. (Eds DS Powlson *et al.*) pp. 181–199. (Springer-Verlag: Berlin).

Multimodeling – An Emerging Approach to Improving Process-Based Modeling of Soil Systems

Yakov Pachepsky[A], Andrey Guber[A], Martinus Th. van Genuchten[B]

[A]Environmental Microbial and Food Safety Laboratory, USDA-ARS Beltsville Agricultural Research Center, Beltsville, MD, USA, Email yakov.pachepsky@ars.usda.gov
[B]Department of Mechanical Engineering, Federal University of Rio de Janeiro, UFRJ, Rio de Janeiro, RJ, 21945-970, Brazil

Abstract
Environmental systems usually are approximated in mathematical terms by making simplifying assumptions that lead to multiple model structures which may produce results that are equally consistent with available observations. An increasing number of papers are now being published on various applications of multimodeling in which predictions from various independent models are combined, rather than attempting to find the best model. Multimodeling consists of assigning weights to the simulation results from the various models, and then combining these results into a single prediction. We constructed a multimodel using 14 independent Richards equation-based individual models by employing different pedotransfer functions. The individual models were not calibrated. Soil water contents were monitored for 300 days with multisensory capacitance probes at eight depths in four locations. Simulations using seven different methods to assign weights to individual models were compared with observed soil water time series. The multimodel was by far more accurate and reliable than the individual models. The concurrent use of several models, and mutimodeling in particular, presents an opportunity to better understand and forecast soil processes.

Key Words
Multimodeling, concurrent use, model weights, soil water, pedotransfer functions.

Introduction
Having a multiplicity of models of the same process or phenomenon is commonplace when modelling environmental processes, especially when the soil-plant-atmosphere system is considered. The multiplicity relates to differences in the simplifications needed to express observed natural complexities in mathematical terms, differences in model emphasis, and differences in scales at which models were developed or the natural system was observed (Beven, 2002). A massive effort in developing criteria for selecting the best model has thus far not produced a univocal solution. All error-based methods condition the evaluation and comparison of models on the available data. Using the reasonability of forecasts to evaluate models, e.g. with the GLUE methodology (Beven and Binley, 1992), does not exclude the subjective element of selecting cutoffs and defining reasonability. Invoking measures of model complexity based on the number of model parameters is problematic for nonlinear models. The uncertainty of the model structure is in most cases difficult to include in the criteria statistics (van Ness and Sheffer, 2005).

The last 10 years has seen a marked interest in making use of different conceptual approaches instead of attempting to find the best model or using a single preferred model. Several approaches to the concurrent use of several models are currently being pursued. One approach is multimodeling, which consists of assigning weights to the simulation results from different models, and then combining results from the individual models into a single prediction (Burnham and Anderson, 2002). Multimodeling has been shown to improve both deterministic and probabilistic performances of predictions (Hagedorn *et al.* 2005). The objective of this work was to investigate and demonstrate the applicability of multimodeling to water flow in variably saturated field soils.

Methods
Multimodeling
The use of the term "multimodel" in publications has grown exponentially during the past ten years. To deal with uncertainties in model selection, multimodel prediction has emerged as a popular technique in climate prediction (Barnston *et al.* 2003), but later propagated also to surface hydrology (e.g., Regonda *et al.* 2006), subsurface hydrology (Neuman, 2002; Guber *et al.* 2009), and ecological modeling (Link and Barker, 2006). Since its introduction, multimodel prediction based on combining results from more than one model has been subject to much debate that can be summarized into two questions: (a) is a multimodel prediction better than the

single best forecast, and (b) what is the best approach to weigh predictions obtained with the different models. The improvement in predictions has been attributed to the fact that the multimodel provides better coverage of system parameter space. The relation between the average capability of the single model and the performance of the multimodel is not linear, especially when the probabilistic diagnostics is considered (Hagedorn *et al.* 2005). Selection of weights in multimodels is currently still a topic of research. Alternative methods for weighing have been reviewed by Armstrong (2001) and Burnham and Anderson (2002), among others. The most often used methods are:

1) arithmetic averaging of results from all models (AA),
2) superensemble forecasting (SF) where the multimodel result is the multiple linear regression with individual forecasts as the independent variables (Krishnamurti *et al.* 2000),
3) superensemble with singular value decomposition (SVD) to alleviate effects of multicollinearity caused by similarity in the predictions of individual models (Kharin and Zwiers, 2002),
4) Bayesian model averaging (BA), (Neuman, 2002),
5) using information theory (IT) to select weights by minimizing the information loss, for example by using Akaike criteria (Poeter and Andersen, 2005), and
6) using weights inversely proportional to the accuracy of each model on a training dataset (IW).

The multimodel in this study was built using 14 individual models. Each of the models employed the Richards flow equation, the Brooks-Corey-Campbell or van Genuchten-Mualem equations for water retention and the unsaturated hydraulic conductivity, and one of 14 pedotransfer functions (PTFs) to estimate the hydraulic parameters from basic soil properties: (1) Rosetta (Schaap *et al.* 2001), (2) Vereecken et al. (1989), (3) Varallyay et al. (1982), (4) Wösten et al. (1999), (5) Rawls and Brakensiek (1982), (6) Saxton et al. (1986), (7) and (8) Williams et al. (1992), (9) Campbell and Shiozawa (1992), (10) Oosterveld and Chang (1980), (11) Mayr and Jarvis (1999), (12) Gupta and Larson (1979), Tomasella and Hodnett (1998), and Rawls et al. (1983). References to these PTF sources are given by Pachepsky et al. (2007), while a computer code to compute water retention according these functions is available upon request from the first author. The saturated hydraulic conductivity of the different textural classes was estimated as described in Pachepsky and Rawls (2004). None of the individual models was calibrated.

Field data

Field data were obtained from a 10x10 m plot at the research site of the Beltsville Agricultural Research Center, Maryland, USA. Soils at the site are classified as a coarse-loamy, siliceous, mesic Typic Hapludult, either well or excessively well drained. On average, the soils have a coarse loamy sand surface horizon (0-25 cm, organic matter 1.2-5.1%), followed by a sandy loam horizon (25-80 cm), and a loam horizon (80-120 cm), with loamy sand and fine-textured clay loam lenses between 120 and 250 cm. Soil water content measurements were taken with multi-sensor capacitance probes, MCPs (EnviroSCAN, SENTEK Pty Ltd., South Australia), at four locations within the plot. Data were recorded each 15 minutes from January 1 through October 23, 2007, at depths from 10 cm to 80 cm at 10 cm increments. The MCPs were connected to a CR-10X datalogger. Collected data were acquired using a Redwing 100 Airlink modem (Campbell Scientific, Inc., Logan, Utah) once a day. Soil texture, bulk density and organic carbon content were measured at each location at depths from 10 cm to 100 cm at 10 cm increments. Rainfall at the site was measured with a pluviograph, while other weather data were obtained from the energy balance meteorological station with an eddy covariance tower located in 100 m from the plot. Daily evaporation rates were estimated using the Pennman-Monteith equation. We used the HYDRUS-1D software for all of the simulations.

Results

Basic soil properties and multimodeling results

Basic soil properties varied substantially across the plot and with depth. Bulk density increased from 1.35-1.55 g/cm^3 at 5 cm depth to 1.70-1.95 g/cm^3 at 90 cm. Sand content varied between 55 and 65 % at the surface and between 50 to 70 % at the 90 cm depth. The organic matter content did not show substantial variability, decreasing exponentially with depth from 2% at 5 cm depth to 0.2 % at 90 cm. The variations in texture and bulk density resulted in differences in the soil water regimes among the different locations (Figure 1). The multimodel provided accurate simulations of the daily average water contents at all depths (Figure 1). The lowest RMSE values were obtained with singular value decomposition (SVD) weighing. RMSEs were within the range of 0.018 cm^3/cm^3 to 0.061 cm^3/cm^3 at the depth of 10 cm, and within the range of 0.005 cm^3/cm^3 to 0.019 cm^3/cm^3 below 10 cm at four locations. The best individual model performed markedly worse than the multimodel.

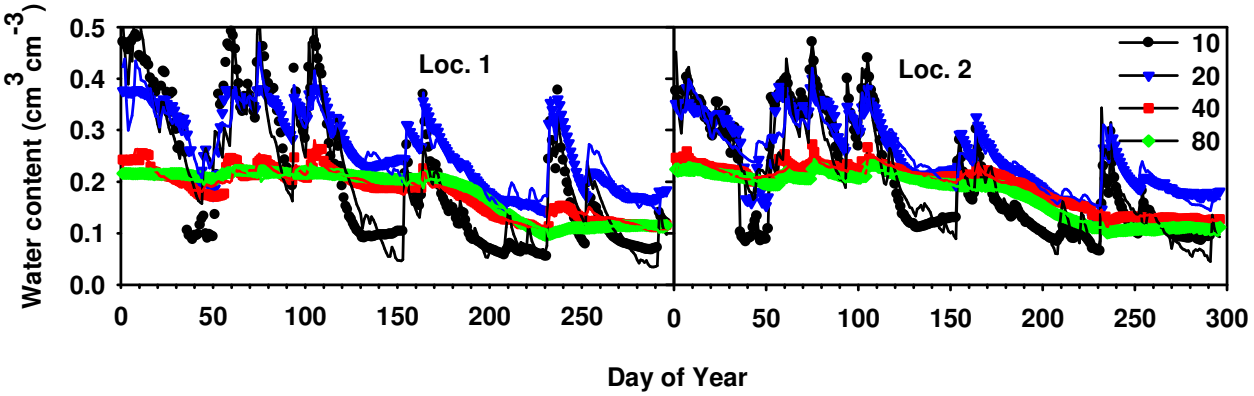

Figure 1. Examples of the multimodel accuracy at different depths at two monitoring locations. Symbols and lines show observed and simulated soil water content time series, respectively; the legend shows depth in cm.

Reliability of multimodeling results

Each water content time series was split into a training and a testing dataset. Training datasets were defined within time windows from 10 to 150 days long, and then moved across the whole observation period. All data outside the windows were used to test the multimodel prediction. The best fit of the multimodel to the daily water contents in the training sets were obtained using weights. The various weighing methods were evaluated in terms of their accuracy and uncertainty (i.e., average and standard deviation) in reproducing the measured water contents of the training datasets (Figure 2).

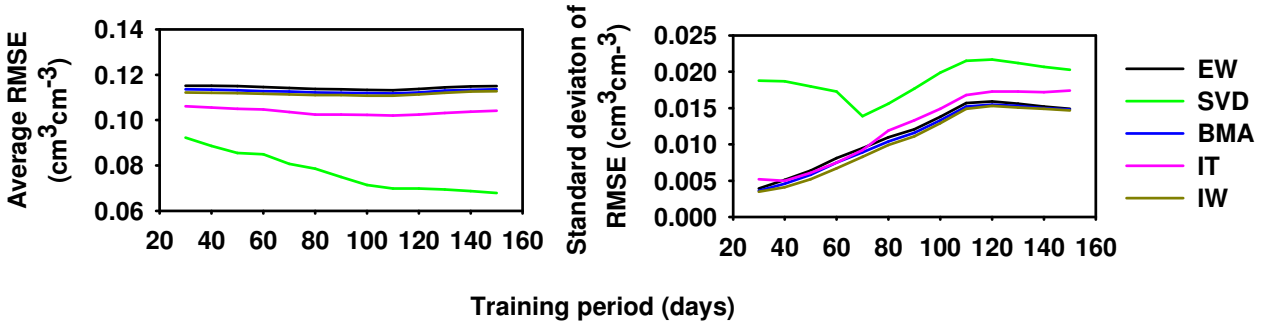

Figure 2. Changes in the multimodel error (RSME) of the test datasets with the duration of the multimodel training period. Colors show different weighting methods; abbreviations are explained in the text.

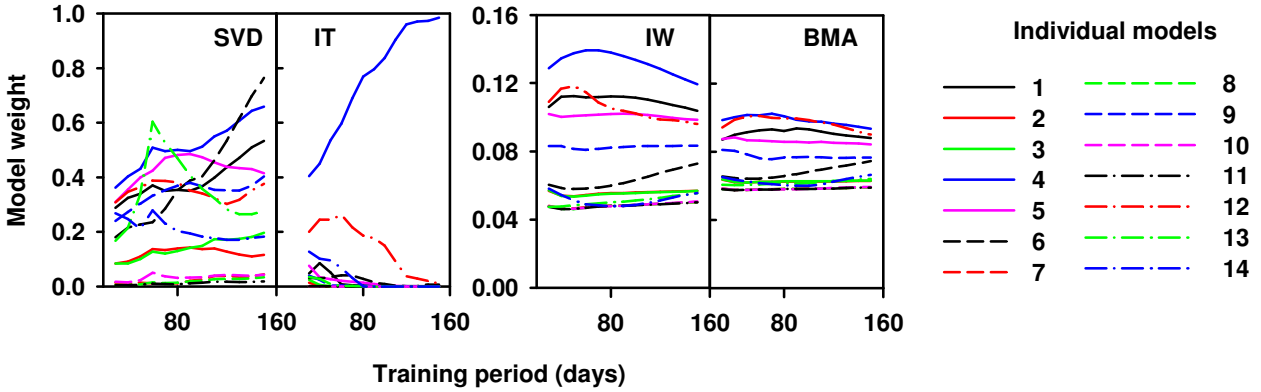

Figure 3. Changes in the weights of individual models with the length of the multimodel training period for the SVD, IT, IW and BMA weighting methods. See text for abbreviations and PTF numbers.

The length of the training period affected the accuracy of the predictions. In most cases, the average RMSE decreased and the standard deviation of the RMSE increased with an increase in the training period for all models and locations. Individual models had different weights at different depths, with the weights of some of the weighting methods also being dependent upon the duration of training period (Figure 3).

Discussion and conclusion

Multimodeling was found to be very effective approach to improving the accuracy of the flow simulations.

Accuracy and reliability of the multimodeling approach in our study varied among the six weighing methods. Overall, the best predictions were obtained with the SVD weighting method, probably because this method is well suited to decrease the effects of the multicollinearity of the inputs from the individual models. The main uncertainty factors were variation in soil properties, and the length of the training period. The reliability of the multimodeling approach increased with the length of the training period.

The excellent results obtained in this study indicate much promise in using the multimodeling methodology for analysing field-scale water flow data. Still, multimodeling is not the only way to take advantage of the concurrent use of existing models. Other approaches, such as model abstraction, have proved to be effective also. Model abstraction systematically simplifies a more complex model into a series of simpler models, and then uses these to (a) learn more about the system, (b) improve robustness of the predictions, (c) improve communication between the modeling results, and (d) improve performance of the modeling system as a whole (Pachepsky *et al.* 2007). Overall, the concurrent use of several models presents an important avenue for improving our understanding of soil processes.

References

Armstrong RA (2001) Combining forecasts. In 'Principles of Forecasting: A Handbook for Researchers and Practitioners'. (Ed. JS Armstrong) pp. 417-439 (Kluwer Academic: Dordrecht)

Barnston AG, Mason S, Goddard L, Dewitt DG, Zebiak SE (2003) Multimodel ensembling in seasonal climate forecasting at IRI. *Bulletin of American Meteorological Society* **84**, 1783–1796.

Beven K (2002) Towards a coherent philosophy for modelling the environment. *Proceedings of the Royal Society A: Mathematical, Physical and Engineering Sciences* **458**, 2465-2484.

Beven K, Binley A (1992) The future of distributed models: model calibration and uncertainty prediction. *Hydrological Processes* **6,** 279-298.

Burnham KP, Anderson DR (2002) Model selection and inference: a practical information-theoretic approach (Springer-Verlag, New York).

Guber AK, Pachepsky YA, van Genuchten MT, Simunek J, Jacques D, Nemes A, Nicholson TJ, Cady RE (2009) Multimodel Simulation of Water Flow in a Field Soil Using Pedotransfer Functions. *Vadose Zone Jourrnal* **8,** 1–10.

Hagedorn R, Doblas-Reyes FJ, Palmer, TN (2005) The rationale behind the success of multi-model ensembles in seasonal forecasting – I. Basic concept. *Tellus* **57A**, 219-233.

Kharin V, Zwiers FW (2002) Climate predictions with multimodel ensembles. *Journal of Climate* **15**, 793-799.

Link WA, Barker RJ (2006) Model weights and the foundations of multimodel inference. *Ecology* **87**, 2626-2635.

Neuman SP (2002) Accounting for conceptual model uncertainty via maximum likelihood Bayesian model averaging. *IAHS-AISH Publication* **277**, 303-313.

Pachepsky YA, Rawls WJ. (2003) Soil structure and pedotransfer functions. *European Journal of Soil Science* **54,** 443-452

Pachepsky YA, Guber AK, van Genuchten MT, Nicholson TJ, Cady RE, Simunek J, Schaap MC (2007) Model abstraction techniques for soil water flow and transport. NUREG/CR-6884. (U.S. Nuclear Regulatory Commission, Washington, D.C.) www.nrc.gov/reading-rm/doc-collections/nuregs/contract/cr6884

Poeter E, Anderson D (2005) Multimodel ranking and inference in ground water modeling. *Ground Water* **43**, 597-605.

Regonda SK, Rajagopalan B, Clark M, Zagona E (2006) A multimodel ensemble forecast framework: Application to spring seasonal flows in the Gunnison River Basin. *Water Resources Research* **42**, W09404, doi:10.1029/2005WR004653.

Van Nes EH, Scheffer M (2005) A strategy to improve the contribution of complex simulation models to ecological theory. *Ecological Modelling* **185**, 153–164.

Realistic quantification of input, parameter and structural errors of soil process models

Gerard B.M. Heuvelink[A]

[A]Environmental Sciences Group, Wageningen University and Research Centre, Wageningen, The Netherlands, Email gerard.heuvelink@wur.nl

Abstract
Error propagation analysis with soil process models requires realistic quantification of errors in model inputs, model parameters and model structure. Once this is achieved, the error propagation analysis itself is relatively straightforward, and can for instance be done by employing a Monte Carlo simulation approach. Input error assessment is often complicated because it must include spatial, temporal and cross-correlations of input errors and must assess these at the right spatio-temporal support. Data-driven methods are preferred, but when data availability is poor, a people-driven method using expert elicitation can be used. Errors in model parameters can best be derived using Bayesian calibration, which requires that sufficient model output observations are available at the right support, and that the calibration procedure accounts for model input and structural errors. Bayesian model averaging is advocated for model structural error quantification, but this will only work when multiple models are available that cover the entire space of plausible models. If this cannot be guaranteed, a more sensible approach is to use a stochastic model that incorporates model structural error as system noise.

Key Words
Pedometrics, expert elicitation, bayesian calibration, bayesian model averaging, stochastic systems theory.

Introduction

Soil scientists know better than anyone else that the outputs of soil process models are not perfect. The reasons are well known: there are errors in the model input, model parameters and model structure. These errors propagate through the model in ways that often cannot easily be predicted without the help of specific tools. Therefore, in the past decades many approaches have been developed, implemented and applied to analyse error propagation in environmental and soil process models (e.g. Hyvonen *et al.* 1998; Bishop *et al.* 2006; Brown and Heuvelink 2007; Castrignano *et al.* 2008; Dean *et al.* 2009; Heuvelink *et al.* 2009). The most flexible and most often used approach is the Monte Carlo method, which is remarkably simple and easily implemented. First, the errors about the various 'inputs' to the model are characterized by probability distributions. Next, a pseudo-random number generator is used to sample from these distributions, and the model is run with the sampled inputs. This process is repeated many times, each time running the model with a new sample of inputs and storing the result. The spread in the so-obtained set of model outputs characterizes the model output error.

Although error propagation analysis with the Monte Carlo method may look simple and straightforward, it turns out to be difficult when concepts are to be put into practice. Important challenges are:

- realistic quantification of error in model inputs, parameters and model structure;
- keeping the required computation time within acceptable bounds;
- ensuring that all important error sources are included in the analysis;
- controlling the Monte Carlo sampling error;
- assessing the contribution of individual error sources to the output error;
- assessing error in spatio-temporal aggregates of model outputs;
- validation of the outcome of an error propagation analysis.

In this paper we only address the first of these challenges, because this is arguably the most crucial problem and space limitations prohibit a comprehensive analysis of all challenges. However, it should be noted that all are important and deserve attention. Also, the list may not be exhaustive.

Realistic quantification of error in model inputs, parameters and model structure

Although the distinction between model inputs and model parameters is not always obvious and models may have 'inputs' that are in the 'grey zone' between input and parameter (e.g. hydraulic conductivity, weathering rate), it is useful to separate error assessment for inputs from that for parameters. Inputs are defined as real-world properties that exist regardless of the model and can in principle be observed. Parameters are only defined

1 – 6 August 2010, Brisbane, Australia. Published on DVD.

within the context of a model and loose their meaning when there is no model (e.g. regression coefficients).

Input error assessment

Probability distributions associated with errors in model inputs can be derived in various ways, such as by analysing replicates in a laboratory to quantify laboratory measurement error, comparison of ground-truth data with mapped data to assess generalisation and classification errors, and use of geostatistics to quantify spatial interpolation error. These 'data-driven' methods are well-developed and are continuously improved, such as in geostatistics where the ordinary kriging paradigm has gradually been replaced by more elaborate approaches such as regression kriging (Hengl *et al.* 2004) and generalized linear models for geostatistical data (Diggle and Ribeiro 2007). Basically, improvement focuses on making more realistic assumptions. For instance, ordinary kriging assumes that the soil property of interest is a realization of a second-order stationary random function that has a constant mean (Webster 2000), whereas regression kriging allows the mean of the soil property to depend on external explanatory variables. Note, however, that assumptions must always be made, because the amount of data is insufficient to uniquely derive the entire probability distribution of the input error, which should include spatial, temporal and cross-correlations when relevant. One important issue that is rarely addressed in data-driven approaches but that needs attention is that the data used to quantify the error in the model input may have non-negligible observation error. Input error will be systematically overestimated if this is ignored. Pedometricians know that the 'support' of the observations is also crucially important when deriving error distributions. For instance, the error associated with the nitrate concentration of the soil solution at a 'point' in space and time is much larger than that associated with the annual average of an entire field because 'hot spots' in time and space will average out over the larger support. Thus, it is imperative that input error quantification is done at the support required by the model (Heuvelink 1998). Data-driven approaches are less developed for categorical soil properties. Only few approaches exist that derive the entire probability distribution of spatially distributed categorical variables (e.g. Finke *et al.* 1999; Hartman 2006; Brus *et al.* 2008), and most of these are cumbersome, make unrealistic assumptions or have severe limitations.

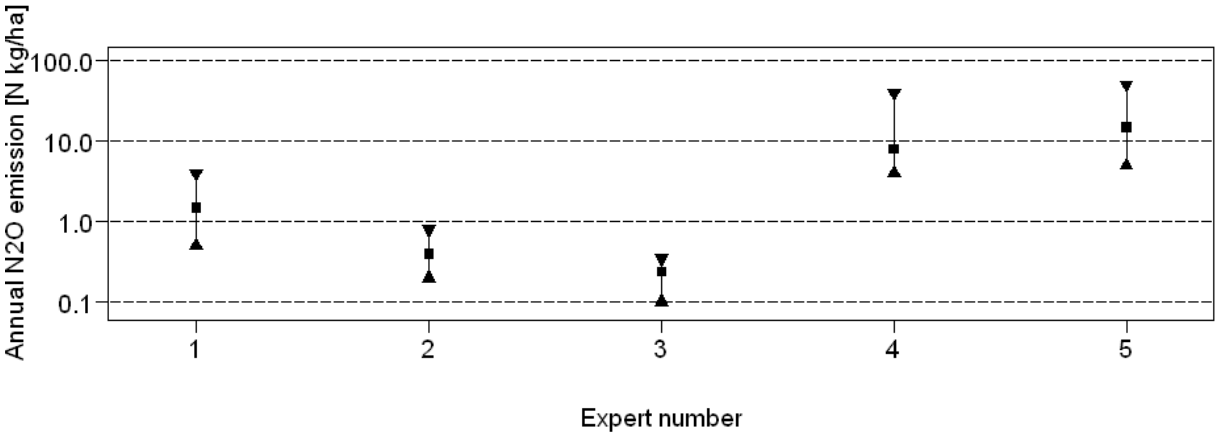

Figure 1. Error in annual N_2O emission (kg N/ha) from 1 ha plots on arable land on clay soils across Europe, independently estimated by five experts. The probability distribution of the error is characterized by the 25 (triangle point up), 50 (square) and 75 (triangle point down) percentiles.

Although the data-driven approach is the preferred option, in many practical cases it may fail for lack of sufficient data, leaving the 'people-driven' approach as the only alternative (Brown and Heuvelink 2005). Here, expert elicitation is used to derive probability distributions of model inputs. As an example, Figure 1 reports the quantified error about the annual nitrous-oxide emission (kg N/ha) for 1 ha plots on arable land on clay soils across Europe, estimated independently by five experts (Shang 2009). There is much disagreement between experts, which makes it difficult to merge their assessments. Figure 1 also shows that it is risky to rely on just one expert, which seems to be the common approach in people-driven assessment of input error (e.g. De Vries *et al.* 2003; Lesschen *et al.* 2007). It is imperative that we learn more about expert elicitation, which is well-developed in the risk analysis literature (e.g. Kaplan 1992; Ayyub 2001; Cooke and Goossens 2004). It must be adapted to the type of applications which pertain to soil science and extended to the quantification of support-dependent spatial- and cross-correlations.

Parameter error assessment

Errors in model parameters can only be realistically assessed by inverse methods, in which model predictions are compared with model output observations and parameter error is assigned such that it explains the observed differences. Common approaches are PEST (http://www.sspa.com/pest/) and GLUE (Dean *et al.* 2009).

Recently, Bayesian calibration was introduced to the environmental sciences and also to soil science (Reinds *et al.* 2007). Starting with user-defined a priori probability distributions, Bayesian calibration uses Markov Chain Monte Carlo methods to update these distributions with information derived from the observations. Bayesian calibration is attractive because it is flexible, mathematically sound, easily implemented, and yields the full joint probability distribution of the model parameters. It is computationally demanding and standard application ignores the contribution of errors in inputs, model structure and parameters not included in the analysis. Also, the decision whether to assume that parameters are constant or variable in space and/or time turns out to be crucial (e.g. Reinds *et al.* 2007). Pedometricians and soil process modellers must take a closer look at these issues and ensure that the methodology is properly applied.

Model structure error assessment
Bayesian calibration has been extended to include model structural error. This is known as Bayesian model comparison or Bayesian model averaging (Raftery *et al.* 1997). Multiple models are considered and each gets assigned a prior probability of being the 'true' model. Next these prior probabilities are updated to posterior probabilities based on the amount of agreement between observed and predicted model outputs. The methodology works well with statistical (regression) models, where a large number of candidate models can easily be formulated simply by including or excluding explanatory variables, but extension to physically-based models is cumbersome. Refsgaard *et al.* (2006) present a framework for dealing with model structural error in hydrological modelling that uses multiple model structures, but acknowledge that the range of models must span the entire space of plausible models. The latter will be difficult in practice, because most models borrow concepts from each other, are built by people that have the same education, meet at conferences and read each others work. In addition, the development of a complex soil process model is a time consuming affair that may involve many man years of work. These are all disadvantages of the Bayesian model averaging approach to soil process modelling. The advantage of Bayesian model averaging is that it can help choosing the optimal degree of model complexity, which is a persistent problem in soil process modelling that as yet has not been satisfactorily resolved.

As an alternative to Bayesian model averaging, we may fall back to models that represent structural errors as (additive) noise terms. This leads to stochastic models or so-called state-space models, for which a rich theory has been developed (e.g. Pugachev and Sinitsyn 2002). Perhaps these models are somewhat restrictive in the way that structural error is represented, but the practical advantages are evident. Also, stochasticity can be defined at the level of the underlying differential equations, which seems physically plausible. The use of stochastic models and associated data assimilation methods, such as ensemble Kalman filtering and particle filtering, is abundant in disciplines such as hydrology, meteorology and oceanography. However, in soil science their use has been very restricted. There is no reason to believe that model structural error is less important in soil science, and if we want to address it thoroughly we need to get more involved in these approaches.

Conclusion
Quantification of error in the inputs, parameters and structure of soil process models needs more attention because model outputs should be accompanied by accuracy measures and realistic assessment of these errors is indispensible for sound error propagation analysis. In this respect, soil science still lags behind compared to other disciplines within the earth and environmental sciences. Most published studies only focus on the propagation of errors in model input, but this is only one component of the total error. Also, input error assessment must benefit more from developments in the expert elicitation literature. Bayesian inverse modelling approaches for quantification of errors in parameters and model structure are useful too, but it is important that these make comparisons at the right support and include all error sources (errors in inputs, parameters, structure and in observations of model output), because otherwise error estimates for individual error sources will be flawed.

References
Ayyub BM (2001). Elicitation of Expert Opinions for Uncertainty and Risks. CRS Press, Florida.

Bishop TFA, Minasny B, McBratney AB (2006). Uncertainty analysis for soil-terrain models. *International Journal of Geographical Information Science* **20**, 117-134.

Brown JD, Heuvelink GBM (2005). Assessing uncertainty propagation through physically based models of soil water flow and solute transport. In 'Encyclopedia of Hydrological Sciences'. (Ed MG Anderson), pp. 1181-1195. (Wiley: Chicester).

Brown JD, Heuvelink GBM (2007). The Data Uncertainty Engine (DUE): a software tool for assessing and simulating uncertain environmental variables. *Computers & Geosciences* **33**, 172-190.

Brus DJ, Bogaert P, Heuvelink GBM (2008), Bayesian Maximum Entropy prediction of soil categories using a traditional soil map as soft information. *European Journal of Soil Science* **59**, 166-177.

Castrignano A, Buttafuoco G, Canu A, Zucca C, Madrau S (2008). Modelling spatial uncertainty of soil erodibility factor using joint stochastic simulation. *Land Degradation & Development* **19**, 198-213.

Cooke RM, Goossens LHJ (2004). Expert judgement elicitation for risk assessments of critical infrastructures. *Journal of Risk Research* **7**, 643-656.

Dean S, Freer J, Beven K, Wade AJ, Butterfield D (2009). Uncertainty assessment of a process-based integrated catchment model of phosphorus. *Stochastic Environmental Research and Risk Assessment* **23**, 991-1010.

De Vries W, Kros J, Oenema O, De Klein J (2003). Uncertainties in the fate of nitrogen II: A quantitative assessment of the uncertainties in major nitrogen fluxes in the Netherlands. *Nutrient Cycling in Agroecosystems* **66**, 71-102.

Diggle PJ, Ribeiro Jr. PJ (2007). 'Model-based Geostatistics'. (Springer: New York).

Finke PA, Wladis D, Kros J, Pebesma EJ, Reinds GJ (1999). Quantification and simulation of errors in categorical data for uncertainty analysis of soil acidification modelling. *Geoderma* **93**, 177-194.

Hartman LW (2006). Bayesian modelling of spatial data using Markov random fields, with application to elemental composition of forest soil. *Mathematical Geology* **38**, 113-133.

Hengl T, Heuvelink GBM, Stein A (2004). A generic framework for spatial prediction of soil properties based on regression-kriging. *Geoderma* **120**, 75-93.

Heuvelink GBM (1998). Uncertainty analysis in environmental modelling under a change of spatial scale. *Nutrient Cycling in Agro-ecosystems* **50**, 255-264.

Heuvelink GBM, Van Den Berg F, Burgers SLGE, Tiktak A (2009). Uncertainty and stochastic sensitivity analysis of the GeoPEARL pesticide leaching model. *Geoderma* **155**, 186-192.

Raftery AE, Madigan D, Hoeting JA (1997). Bayesian model averaging for linear regression models. *Journal of the American Statistical Association* **92**, 179-191.

Hyvonen R, Agren GI, Bosatta E (1998). Predicting long-term soil carbon storage from short-term information. *Soil Science Society of America Journal* **62**, 1000-1005.

Kaplan S (1992). Expert information versus expert opinions - another approach to the problem of eliciting combining using expert knowledge in probabilistic risk analysis. *Reliability Engineering & System Safety* **35**, 61-72.

Lesschen JP, Stoorvogel JJ, Smaling EMA, Heuvelink GBM, Veldkamp A (2007). A spatially explicit methodology to quantify soil nutrient balances and their uncertainties at the national level. *Nutrient Cycling in Agro-ecosystems* **78**, 111-131.

Pugachev VS, Sinitsyn IN (2002). 'Stochastic Systems: Theory and Applications'. (World Scientific Publishing: Singapore).

Refsgaard JC, Van Der Sluijs JP, Brown J, Van Der Keur P (2006). A framework for dealing with uncertainty due to model structure error. *Advances in Water Resources* **29**, 1586-1597.

Reinds GJ, Van Oijen M, Heuvelink GBM and Kros H (2008). Bayesian calibration of the VSD soil acidification model using European forest monitoring data. *Geoderma* **146**, 475-488.

Shang H (2009). Estimation of terrestrial greenhouse gas emissions in Europe. MS thesis, Wageningen University.

Webster R (2000). Is soil variation random? *Geoderma* **97**, 149-163.

Saturation-dependent anisotropy of unsaturated soils

Jianting Zhu[A] and Dongmin Sun[B]

[A]Desert Research Institute, Nevada System of Higher Education, Las Vegas, Nevada, USA, Email Jianting.Zhu@dri.edu
[B]University of Houston-Clear Lake, Environmental Science, Houston, Texas, USA, Email sundon@uhcl.edu

Abstract
The effect of saturation degree on hydraulic conductivity anisotropy in unsaturated soils is still an outstanding issue. This study investigates the impact of soil texture and soil bulk density on the degree of saturation-dependent anisotropy of layered soils by combining pedo-transfer function (PTF) results with the thin layer concept. The main objective is to examine how anisotropy characteristics are related to the relationships between hydraulic properties and the basic soil attributes such as texture and bulk density. The hydraulic parameters are related to the texture and bulk density based on the PTF results through linear regression. The results illustrate that the coupled dependence of the hydraulic parameters on the texture and bulk density is important to determine the anisotropic behavior and the inter-relationships of soil texture, bulk density, and hydraulic properties may cause very different saturation-dependent of unsaturated soils.

Key Words
Arithmetic mean, harmonic mean, anisotropy factor, capillary pressure, minimum anisotropy.

Introduction

Large scale heterogeneous soils often demonstrate different moisture spreading and solute transport patterns at different saturation degrees (or capillary pressure head levels). While saturation-dependent anisotropy has been recognized for a long time (e.g., Zaslavsky and Sinai, 1981; Stephens and Heerman, 1988), is has not been fully understood. Mualem (1984) proposed a conceptual model to quantify the capillary pressure-dependent anisotropy by assuming that soils consist of many thin layers**.** A similar concept was extended to consider effects of bulk density variations within a particular soil type (Assouline and Or, 2006). Other approaches have also been proposed to study the soil anisotropy behavior. Zhang *et al*. (2003) proposed a tensorial connectivity-tortuosity concept to describe the unsaturated soil hydraulic conductivities. McCord *et al*. (1991) described a series of soil water tracer experiments and approaches to numerically model the flow behavior observed in field experiments. These experimental and numerical results provided strong supporting evidence for a variable, saturation-dependent anisotropy in the hydraulic conductivity of an unsaturated medium. Green and Freyberg (1995) calculated the capillary pressure-dependent anisotropy under conditions of large-scale gravity drainage. Ursino *et al*. (2000) used Miller similitude with different pore-scale geometries of the basic element to model macroscopic flow and transport behavior. Their results demonstrated that the geometry of the microstructure could lead to anisotropic behavior at larger scale even if the system is characterized by an isotropic correlation structure. Khaleel *et al*. (2002) used a unit-mean-gradient approach to derive upscaled hydraulic properties for flow parallel and perpendicular to bedding by simulating steady gravity drainage conditions for a series of applied infiltration rates of relatively dry conditions in coarse-textured sediments. In this study, we investigate unsaturated soil anisotropy that arises from a combination of soil texture and bulk density variations and the pedo-transfer function (PTF) results of soil hydraulic conductivities. PTFs transform basic soil properties such as texture and bulk density into water retention and unsaturated hydraulic conductivity. The main objective is to improve the fundamental understanding of various saturation-dependent anisotropy behaviors. Specifically, we examine how different inter-relationships of soil texture, bulk density and hydraulic properties may induce different anisotropy characteristics.

Methods

Hydraulic properties in relation to texture and bulk density

Van Genuchten (1980) combined the soil water retention function with the statistical pore-size distribution model and obtained the following hydraulic property functions,

$$Se = [1 + (\alpha h)^n]^{-m} \quad (1)$$

$$K = K_S[1 - (1 - Se^{1/m})^m]^2 \quad (2)$$

where $Se = (\theta-\theta_r)/(\theta_s-\theta_r)$ is the effective degree of saturation, θ is the volumetric water content, θ_r is the residual volumetric water content, θ_s is the saturated volumetric water content, h is the capillary pressure head, K is the hydraulic conductivity, K_S is the saturated hydraulic conductivity; α, m and n are empirical hydraulic shape

parameters, and m=1-1/n. Based on the results of the van Genuchten hydraulic parameters in relation to texture (using mean grain diameter d as a surrogate) and the bulk density established by the neural network based PTFs (Schaap and Leij, 1998) (see Table 1), we perform regression analyses to establish empirical linear relationships, which relate hydraulic properties to the two main indicators, the grain diameter d and the bulk density ρ.

Table 1: Mean soil grain diameters, average hydraulic parameters and bulk density values for the soil textural classes (Hydraulic parameters values are from Schaap and Leij (1998))

Class	d (mm)	ρ (g/cm^3)	log(α) (log(1/cm))	log(n)	log(K_S) (log(cm/d))
Sand	0.9249	1.53	-1.45	0.50	2.81
Loamy Sand	0.8245	1.52	-1.46	0.24	2.02
Loam	0.4211	1.37	-1.95	0.17	1.08
Sandy Loam	0.6222	1.46	-1.57	0.16	1.58
Silt Loam	0.2214	1.28	-2.30	0.22	1.26
Sandy Clayey Loam	0.6197	1.57	-1.68	0.12	1.12
Silty Clayey Loam	0.1177	1.32	-2.08	0.18	1.05
Clay Loam	0.4186	1.42	-1.80	0.15	0.91
Silt	0.0747	1.33	-2.18	0.22	1.64
Clay	0.2114	1.39	-1.82	0.10	1.17
Sandy Clay	0.51601	1.59	-1.48	0.08	1.06
Silty Clay	0.11644	1.36	-1.79	0.12	0.98

From the linear regression analyses, it was found that log(n) is poorly correlated to either d or ρ. Hills *et al.* (1992) showed that the variability of soil hydraulic characteristics could be adequately modeled using a variable van Genuchten α with a deterministic van Genuchten n. Therefore, we use the mean value of n in this study. log(α) is best correlated to ρ, and is also fairly correlated to d. The best linear regression is:

$$\log(\alpha) = 0.262d + 1.887\rho - 4.603 \quad (3)$$

where α is in (1/cm), ρ is in (g/cm^3) and d in (mm). The correlation coefficient for this empirical regression relationship is 0.91.

log(K_S) is poorly correlated to ρ, and is fairly correlated to d. The best linear regression relationship is:

$$\log(K_S) = 1.272d + 0.851 \quad (4)$$

where K_S is in (cm/day). The correlation coefficient for this regression relationship is 0.66.

These empirical linear regression relationships are used to develop anisotropy models in the following section. While other non-linear regression relationships or more complicated relationships can also be easily incorporated, we use these linear regression relationships for the sake of simplicity because our goal is to focus on whether and how the inter-relationships of soil texture, bulk density, and hydraulic properties may affect the anisotropy behaviors of layered unsaturated soils.

Anisotropy model

We consider a soil consisting of a large number of thin, but distinguishable layers of different texture (as indicated by d) and the bulk density ρ. Each layer is characterized by its own van Genuchten hydraulic conductivity function, K(Se, K_S, α, n). Since the van Genuchten parameters have been related to d, and ρ as described in the previous section, the hydraulic conductivity can now be written in a general form of K(Se, d, ρ). The layered formation is expressed in terms of a joint probability density function, f(d, ρ), of the grain diameter d and the bulk density ρ. Parallel to the layering, the hydraulic conductivity K_H(Se), is described by the arithmetic mean of K(Se, d, ρ) of the layers (Mualem, 1984; Assouline and Or, 2006),

$$K_H(Se) = \iint K(Se,d,\rho) f(d,\rho) \, dd\rho \quad (5)$$

The hydraulic conductivity perpendicular to the layers, K_N(Se), is described as the harmonic mean of K(Se, d, ρ) of the layers, which is expressed as follows,

$$K_N(Se) = \left[\iint \frac{f(d,\rho)}{K(Se,d,\rho)} dd\rho \right]^{-1} \quad (6)$$

The anisotropy factor, A, can then be expressed as the ratio of the hydraulic conductivities in the parallel and perpendicular directions,

$$A(Se) = K_H(Se)/K_N(Se) \quad (7)$$

For simplicity, we use uniform distributions to describe the probability distributions of both d and ρ, although

other distributions could also be incorporated. Based on the probability density functions and the established regression relationships, we can calculate K_H (hydraulic conductivity parallel to the layering), K_N (hydraulic conductivity perpendicular to the layering), and A (anisotropy factor) as functions of the effective saturation degree Se from Eqns. (5) through (7), which can also be related to the capillary pressure head h.

Results and Discussion

Since K_S is fairly correlated only to the texture (with d as a surrogate), we first consider the case when K_S is related to d and α is related to both d and ρ through the regression relationships shown in Eqn. (4) and Eqn. (3) respectively. Figure 1 shows the relationships between the anisotropy factor A, and h as well the saturatin degree Se for various combinations of d and ρ ranges and n=1.59. Since K_S is not as good as α in terms of correlation to either d and ρ, we also investigate the scenario that a simple constant K_S value equal to the mean value is used and α is related to both d and ρ. Figure 2 shows the relationships between the anisotropy factor A, and h as well Se for this scenario under otherwise same conditions as in Figure 1.

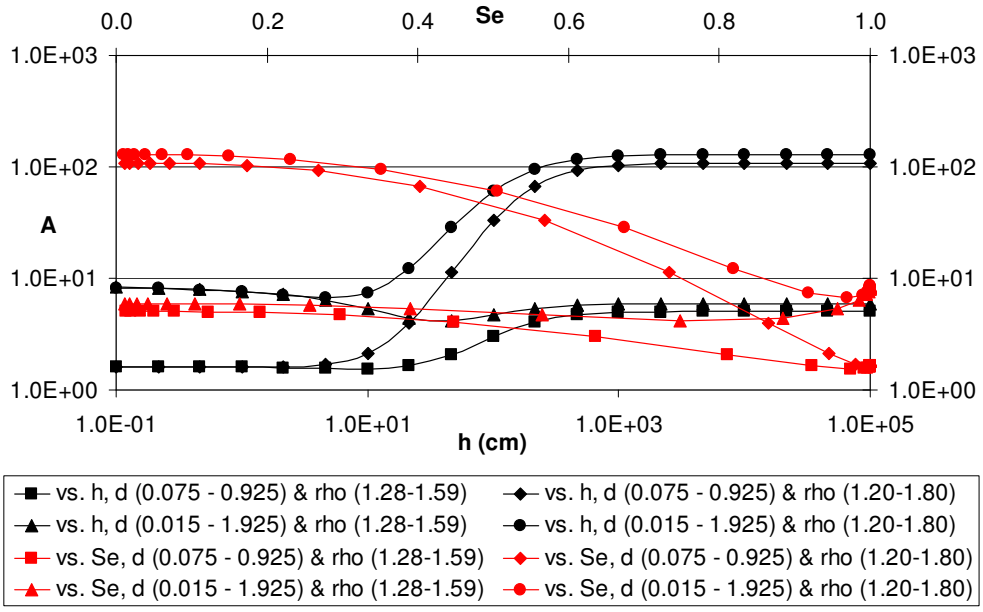

Figure 1. Relationships between the anisotropy factor A and the saturation degree Se as well as the capillary pressure head h. K_S is related to d and α is related to both d and ρ through regression relationship for various combinations of d and ρ ranges. n=1.59.

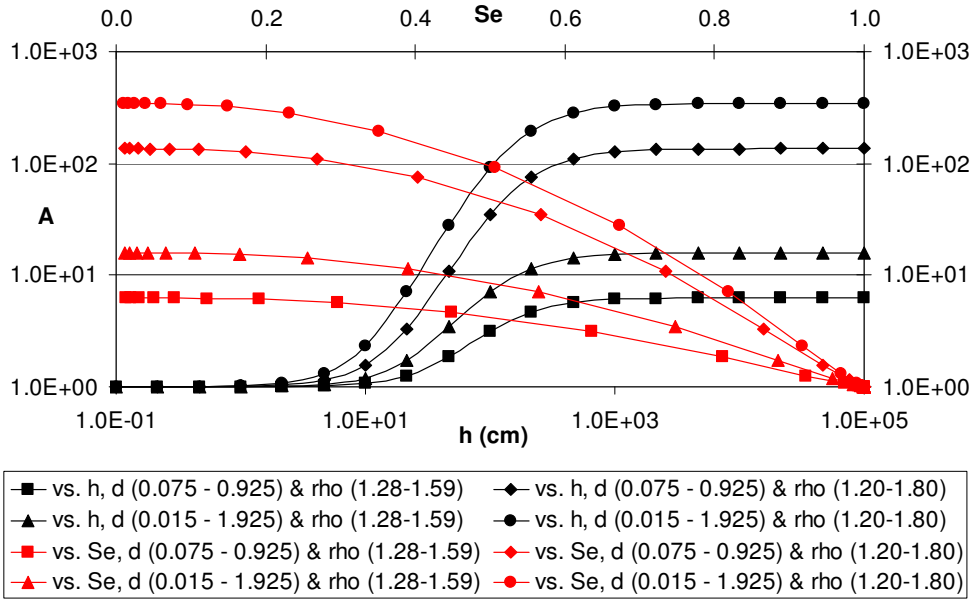

Figure 2. Relationships between the anisotropy factor A and the saturation degree Se as well as the capillary pressure head h. K_S is constant equal to the mean and α is related to both d and ρ through regression relationship for various combinations of d and ρ ranges. *n* = 1.59.

Results shown in Figures 1 and 2 indicate that anisotropy typically increases when the saturation degree decreases (or the capillary pressure head increases). When the grain diameter range is large (i.e., the heterogeneity is strong) and when K_S is related to d, and α is related to both d and ρ, a feature that the anisotropy factor A exhibits a minimum value at certain capillary pressure head (i.e., a non-monotonic relationship) is observed (black triangle symboled curve in Figure 1). Many previous studies (McCord *et al*. 1991; Green and Freyberg, 1995; Assouline and Or, 2006) reported that the soil anisotropy first decreases as the capillary pressure increases and then increase as the capillary pressure further increases (i.e., the anisotropy reaches a minimum at a certain capillary pressure level). Other studies (e.g., Ursino *et al*. 2000; Khaleel *et al*. 2002) found that the soil anisotropy increases monotonically with increasing capillary pressure. This study illustrates that the anisotropy reaches a minimum only when both K_S and α are variables across the soil layers and the heterogeneity of soil attributes across layers is large. For other conditions, the anisotropy is found to increase monotonically with the decreasing saturation degree (or increasing capillary pressure head).

Conclusion

The key conclusions from this study include: 1) the coupled dependence of the hydraulic parameters on the texture and bulk density is important to determine the anisotropic behavior of unsaturated soils, and 2) the inter-relationships of soil texture, bulk density, and hydraulic properties may cause very different anisotropy behaviors of layered unsaturated soils.

References

Assouline S, Or D (2006) Anisotropy factor of saturated and unsaturated soils. *Water Resources Research* **42**, W12403, doi: 10.1029/2006WR005001.

Green TR, Freyberg DL (1995) State-dependent anisotropy - comparisons of quasi-analytical solutions with stochastic results for steady gravity drainage. *Water Resources Research* **31**(9), 2201-2211.

Hills RG, Hudson DB, Wierenga PJ (1992) Spatial variability at the Las Cruces trench site. p. 529–538. In (ed MTh van Genuchten) 'Indirect Methods for Estimating the Hydraulic Properties of Unsaturated Soils'. (University of California Riverside, Riverside, CA).

Khaleel R, Yeh TCJ, Lu Z (2002) Upscaled flow and transport properties for heterogeneous unsaturated media. *Water Resources Research* **38(5)**, 1053 doi: 10.1029/2000WR000072.

McCord JT, Stephens DB, Wilson JL (1991) Hysteresis and state-dependent anisotropy in modeling unsaturated hillslope hydrologic processes. *Water Resources Research* **27**(7), 1501-1518.

Mualem Y (1984) Anisotropy of unsaturated soils. *Soil Science Society of America Journal* **48**, 505-509.

Schaap MG, Leij FJ (1998) Database-related accuracy and uncertainty of pedotransfer functions. *Soil Science* **163**(10), 765-779.

Stephens DB, Heermann S (1988) Dependence of anisotropy on saturation in a stratified sand. *Water Resources Research* **24**(5), 770-778.

Ursino N, Roth K, Gimmi T, Flühler H (2000) Upscaling of anisotropy in unsaturated Miller-similar porous media. *Water Resources Research* **36**(2), 421-430.

van Genuchten MTh (1980) A closed-form equation fro predicting the hydraulic conductivity of unsaturated soils. *Soil Science Society of America Journal* **44**, 892-898.

Zaslavsky D, Sinai G (1981) Surface hydrology: III-Causes of lateral flow. *Journal of Hydraulic Division, ASCE* **107(HY1)**, 37-52.

Zhang, ZF, Ward, AL, Gee GW (2003) A tensorial connectivity-tortuosity concept to describe the unsaturated hydraulic properties of anisotropic soils. *Vadose Zone Journal* **2**, 313-321.